



# FIRE-RES

Innovative technologies & socio-ecological-economic solutions for fire resilient territories in Europe

## D5.5 Extreme Wildfire Events impact and risk estimation module

[www.fire-res.eu](http://www.fire-res.eu)

[fire-res@ctfc.cat](mailto:fire-res@ctfc.cat)

**Project Acronym:** FIRE-RES

**Project name:** Innovative technologies and socio-ecological-economic solutions for fire resilient territories in Europe

**Call ID:** H2020-LC-GD-1-1-2020 (Preventing and fighting extreme wildfires with the integration and demonstration of innovative means)

**Work Package:** 5

**Task Number:** 5.3

**Lead beneficiary:** TSYLVA

**Contributing beneficiary(ies):** TSYLVA



This document was produced under the terms and conditions of Grant Agreement No. 101037419 of the European Commission. It does not necessarily reflect the view of the European Union and in no way anticipates the Commission's future policy in this area.

## Publication

---

**Publication date:** 02/12/2024

**Authors:** Adrián Cardil, Miguel Mendes, Adrián Jiménez-Ruano, Fernando Bezares, TSYLVA;

**Abstract:** This deliverable presents several analyses of the impact and risk of Extreme Wildfire Events (EWEs) using its main drivers and the FireSim module preparation. The analysis focuses on fire radiative power (FRP), rate of spread, wind speed, atmospheric instability, and pyro cumulus/pyro cumulonimbus occurrence. Shrublands have the highest energy release in low severity wildfires, while grassland has lower energy release. Rate of spread increases under unstable atmospheric conditions, especially when the lifted index is between -6 and -2. The Convective Flag was proposed to improve operational adoption efforts. In turn, the FireSim module was updated with an adjusted ROS formulation, affecting both deterministic and probabilistic simulations. Finally, Weather Research and Forecasting (WRF) was employed to provide daily high-resolution meteorological predictions for the four Living Labs, ending with 12 territorial FireRisk metrics visualised on the Integrative Software System (ISS).

**Key words:** fire radiative power, fire behaviour, fire simulation, extreme wildfire events

**Quote as:** Cardil, A., Mendes, M., Jiménez-Ruano, A., Bezares, F. (2024). FIRE-RES EWE impact and risk estimation module. Deliverable D5.5 FIRE-RES project. 62 pages. DOI: 10.5281/zenodo.14215113

**DOI:** [10.5281/zenodo.14215113](https://doi.org/10.5281/zenodo.14215113)

## Dissemination level

---

[X] PU- Public: must be available in the website

[ ] CO- Confidential: Only for members of the Consortium and the Commission Services

[ ] CI – Classified: As referred in to Commission Decision 2001/844/EC

## Document history

---

Edition	Date	Status	Author
<b>Version 1</b>	31/10/2024	Draft	Adrián Cardil, Miguel Mendes, Adrián Jiménez-Ruano, Fernando Bezares (TSYLVA).
<b>Version 2</b>	15/11/2024	Draft Revision1. Ready for QA review 2.	Martín, Senande (MITIGA), Adrián, Jiménez-Ruano (TSYLVA)

<b>Version 3</b>	21/11/2024	Draft Revision 2. Ready for QA review 3.	Erico, Kutchartt (CTFC), Adrián, Jiménez-Ruano (TSYLVA)
<b>Version 4</b>	2/12/2024	Final version ready for submission.	Taüll, Marc (CTFC), Adrián, Jiménez-Ruano (TSYLVA)

Copyright © All rights reserved. This document or any part thereof may not be made public or disclosed, copied or otherwise reproduced or used in any form or by any means, without prior permission in writing from the FIRE-RES Consortium. Neither the FIRE-RES Consortium nor any of its members, their officers, employees or agents shall be liable or responsible, in negligence or otherwise, for any loss, damage or expense whatever sustained by any person as a result of the use, in any manner or form, of any knowledge, information or data contained in this document, or due to any inaccuracy, omission or error therein contained.

All Intellectual Property Rights, know-how and information provided by and/or arising from this document, such as designs, documentation, as well as preparatory material in that regard, is and shall remain the exclusive property of the FIRE-RES Consortium and any of its members or its licensors. Nothing contained in this document shall give, or shall be construed as giving, any right, title, ownership, interest, license or any other right in or to any IP, know-how and information.

The information and views set out in this publication does not necessarily reflect the official opinion of the European Commission. Neither the European Union institutions and bodies nor any person acting on their behalf, may be held responsible for the use which may be made of the information contained therein.

# Table of contents

<b>ACRONYMS</b> .....	<b>4</b>
<b>1.INTRODUCTION</b> .....	<b>6</b>
1.1. Objectives and structure of this deliverable.....	6
<b>2.SIMULATION OF EWES IN THE OPERATIONAL CONTEXT</b> .....	<b>9</b>
<b>3.METHODOLOGY</b> .....	<b>10</b>
3.1. Fire Radiative Power analysis .....	10
3.1.1. <i>Relationships between FRP, surface fuel types and burn severity</i> .....	13
3.1.2. <i>FRP vs Weather metrics</i> .....	19
3.2. ROS vs Weather metrics (Wind Speed) and Atmospheric instability metrics (Lifted Index, Convective Flag) .....	23
3.3. Pyrocumulous presence.....	28
3.4. Methodology transference to European scenario.....	31
<b>4. IMPLEMENTATION</b> .....	<b>36</b>
4.1. FireSim updated model including lifted index .....	36
4.2. Validation of wildfire simulations under unstable conditions.....	36
4.3. FireRisk and FireSim apps implementation .....	39
4.3.1. <i>Living labs description and scenarios data</i> .....	40
4.3.2. <i>Living labs meteorology data</i> .....	42
4.3.3. <i>FireRisk assessment implementation process</i> .....	48
4.3.4. <i>FireSim implementation process</i> .....	55
<b>5. TECHNOLOGY READINESS LEVEL (TRL)</b> .....	<b>58</b>
<b>6. CONCLUSIONS</b> .....	<b>59</b>
<b>7. REFERENCES</b> .....	<b>60</b>

## Acronyms

**AGL:** Above Ground Level

**API:** Application Programming Interface

**BLOB:** Binary Large Object

**CAPE:** Convective Available Potential Energy

**CCL:** Cloud Cover Layer

**CNRS:** Department d'Interior – Generalitat de Catalunya

**CSI:** Critical Success Index

**DB:** Data Bases

**DFMC:** Dead Fuel Moisture Content

**DNB:** Day/Night Band

**DSS:** Decision Support Systems

**EAA:** Extended Attack Assessment

**ECMWF:** European Centre for Medium-Range Weather Forecasts

**EDDI:** Evaporative Demand Drought Index

**EWE:** Extreme Wildfire Event

**FBI:** Fire Behaviour Index

**FMC:** Fuel Moisture Content

**FRP:** Fire Radiative Power

**FWI:** Fire Weather Index

**GFS:** Global Forecast System

**GIS:** Geographic Information System

**GPI:** Growth Potential Index

**GUI:** Graphical User Interface

**JPSS:** Joint Polar Satellite System

**HPC:** High-Performance Computer

**HRRR:** High-Resolution Rapid Refresh

**IAA:** Initial Attack Assessment

**IA:** Innovative Action

**ISS:** Integrative Software System

**ISP:** Integrative System Platform

**LFMC:** Live Fuel Moisture Content

**LSM:** Land Surface Model

**LCL:** Lifted Condensation Level

**LFC:** Level of Free Convection

**LLs:** Living Labs

**MODIS:** Moderate Resolution Imaging Spectroradiometer

**NetCDF:** Network Common Data Form

**NIFC:** National Interagency Fire Center

**NIPV:** Nederlands Instituut Publieke Veiligheid

**NPP:** National Polar-orbiting Partnership

**PFT:** Pyrocumulonimbus Firepower Threshold

**PBL:** Planetary Boundary Layer

**POD:** Probability of Detection

**PyroCb:** Pyrocumulonimbus clouds

**PyroCu:** Pyro cumulous clouds

**QPF:** Quantitative Precipitation Forecasts

**ROS:** Rate of Spread

**SPEI:** Standardised Precipitation-Evapotranspiration Index

**SPI:** Standardized Precipitation Index

**SR:** Success Ratio

**TRL:** Technology Readiness Level

**TSYLVA:** Technosylva

**USGS:** United States Geological Survey

**UNIPD:** Università degli Studi di Padova

**VIIRS:** Visible Infrared Imaging Radiometer Suite

**WFA:** Wildfire Analyst

**VPD:** Vapour Pressure Deficit

**WRF:** Weather Research and Forecasting

# 1. Introduction

This document addresses the work that has been carried out in task “5.3 Modelling and decision support system tools” and is specific to subtask “5.3.1. Extreme forest fire behaviour modelling”. This task aims at improving fire modelling systems to more accurately estimate the EWE behaviour to later enhance early warnings through indexes derived from modelling and implement services to estimate the impact of EWE on direct losses, including the number of buildings and people affected. The specification and development of the fire-atmosphere CNRS ForeFire pyro convective simulator is done in Deliverable D5.3, while this deliverable D5.5 focuses on the tools implemented by TSYLVA, specifically its FireSim simulator, the High-Resolution surface weather forecast (WRF), and risk calculation. For this deliverable, the specific subtask has been addressed at regional and national scales by incorporating high fidelity forecasted weather, atmosphere stability data, and high-resolution fuel data. Based on the results of the previously mentioned subtask, the report also provides the methodology developed to meet the requirements and specifications of the proposed Integrative Software System that is being implemented in subtask “5.1.3. Demonstration of an integrative software system for estimating the EWEs risk and impact in real-time with HR weather data (IA 5.1)”. Furthermore, it provides the implementation of the three main products, that are FireSim, the addition of High-Resolution WRF weather data and the estimation of daily FireRisk metrics (section 4 of the present document).

The methodology process developed and implemented in this deliverable has enabled the materialisation of improved simulation, risk prediction and impacts associated with the EWEs.

## 1.1. Objectives and structure of this deliverable

WP5 of FIRE-RES aims to provide advanced technological solutions, equipment, and decision support systems (DSS) to stakeholders dealing with EWEs in Europe. Task 5.1 focuses on the development of an integrative software system to support EWE decision-making. Subtask 5.3.1 strives to improve fire modelling to evaluate EWE behaviour more precisely. This subtask aims at enhancing fire modelling systems to more accurately estimate the EWE behaviour to later improve early warnings through indexes derived from modelling and implement services to estimate the impact of EWE. As has been specified in deliverable D5.1 (Mendes et al., 2022) and documented in this deliverable D5.5., the development and implementation of wildfire simulation services based on the operational simulation capabilities of Wildfire Analyst from Technosylva has been included, in specific on the fire simulation capabilities from the FireSim wildfire simulator, as well as daily-hourly FireRisk services.

This deliverable D5.5 collects the efforts made to improve the current simulator tool (FireSim), in terms of enhancing the behaviour of the EWEs. This aspect was materialised by an adjustment of the rate of spread (ROS) by including the lifted index, an indicator directly related to convective processes. On the other hand, the incorporation of innovative fire danger indexes was made (such as the Initial Attack Assessment - IAA and the Extended Attack Assessment - EAA) to better estimate the probability of a fire exceeding fire suppression capability (IAA) and to inform end-users of EWE fire behaviour potential in an ongoing wildfire event (EAA).

Another goal was to enable the output of high spatial resolution meteorology of daily risk, which through its injection into FireSim allows its operational use. In addition, to complement the risk layers, data on potentially threatened populations, buildings, vegetation fuel, among others, have been added. All this set of information ultimately seeks to improve the prediction of potential and ongoing EWEs. Therefore, as a summary, the tools and solutions finally implemented both in the FireSim and FireRisk modules, as well as in the FIRE-RES Integrated System (IS), are encompassed in three blocks:

- FireSim was implemented in the addressed Living Labs.
- Daily FireRisk forecast metrics at the level of each addressed Living Lab.
- High-resolution weather (WRF) for each addressed Living Lab.

This deliverable provides a description of the analyses conducted to estimate the impact and risk of Extreme Wildfire Events (EWEs). From a modelling perspective, a diverse number of factors that trigger these extreme fire events are separately analysed, as well as the FireSim module preparation. The methodology and main results are developed in the following sections. Regarding the structure of the deliverable itself, the document is organised as follows:

- **Section 1**, introduces the present document, the addressed work, the FIRE-RES project, the main objectives, as well as the structure of the deliverable.
- **Section 2**, describes the challenges in terms of simulating the EWEs in the operational context.
- **Section 3**, develops the different analyses conducted regarding the main EWEs factors, such as fire radiative power (FRP), rate of spread versus wind speed, atmospheric instability, and pyro cumulus-pyro cumulonimbus occurrence.
- **Section 4**, presents the final implementation of the previous analyses, focusing on the FireSim and FireRisk modules: update of fire simulation model, living labs scenarios and meteorology data preparation as well as the FireSim and FireRisk technical and development processes.
- **Section 5**, details the Technology Readiness Level (TRL) reached.
- **Section 6**, summarises the main conclusions of the present document.

It is important to note that the majority of analyses of the EWEs drivers have been conducted employing data collected from United States databases, due to restrictions and limitations in the context of the European Union. However, for the transference to

the European scenario, weather data derived from ERA5 Copernicus Climate Change Service was employed. In the case of the Weather Research and Forecasting (WRF) grids implementation as well as the Living Labs (LL) scenarios' preparation, different European patterns data sources were used. Both the IAA and EAA indexes are both implemented in different European LLs.

## 2. Simulation of EWEs in the operational context

In the context of the FIRE-RES project, several experimental studies have been conducted regarding EWEs simulation improvements. The range of methodologies is diverse, such as using a fire-atmosphere coupled model (Filippi et al., 2009; Filippi et al., 2011), considering simultaneously fire behaviour forest dynamics and allocation of management action (Gonzalez-Olabarria et al., 2023) and integrated fire simulation approaches to locate firebreaks on the landscape (Recasens et al., 2022). Campos et al. (2023) modelled the pyro-convection phenomenon investigating large-scale meteorological conditions that affected Portugal during the fire season in October 2017.

In this deliverable, the effort carried out for the improvement and adaptation of the fire simulation model to the convective phenomenon of EWEs has been made by means of a rate of spread adjustment, which involves the addition of convection factor (i.e., lifted index). This addition or implementation is indeed going to enhance the expected fire behaviour (or risk) of the EWEs with a prediction of a few hours ahead. It is important to highlight that convective conditions have never been included at the operational level until now; instead, most fire decision-making and dispatch systems often rely on the world-wide employed Fire Weather Index (FWI) and its components. Although the average FWI may be adequate to predict the monthly number of fires in certain regions, accurate FWI prediction does not translate into accuracy in the forecast of fire activity from local to global scales (Di Giuseppe et al., 2020; Ntinopoulos et al., 2022) and cannot be used to estimate fire behaviour and spread. Moreover, one shortcoming of the FWI is that only surface weather conditions are considered (Pinto et al., 2020); thus, it cannot be directly applied solely in the fire danger rating systems to predict the occurrence of EWEs, even more so including pyro convection phenomena.

### 3. Methodology

This section describes different analyses focused on the assessment of EWEs main drivers. Taking into account the consensus shared by the scientific community on the main metrics that trigger, foster and characterise these extreme events, the energy released by the EWEs by means of the fire radiative power (FRP), the relationship between the rate of spread (ROS) and wind speed, the main role of atmospheric instability and finally the pyro cumulus-pyro cumulonimbus occurrence have been assessed.

#### 3.1. Fire Radiative Power analysis

The aim of this analysis is to understand and describe the behaviour of Extreme Wildfire Events (EWE) relating energy liberation (Fire Radiative Power, FRP) with surface fuel types and burn severity. Large and extreme wildfires from the years 2020, 2021 and 2022 were selected to get these relationships. This selection was based on their size, relevance, impact, severity and data availability (Table 1).

*Table 1 List of wildfire events selected from 2020 to 2022*

	2020	2021	2022
<b>Fires</b>	Holiday Farm	Dixie	Mosquito
	Archie Creek	Caldor	Mckinney
	Lions Head	Bootleg	
	North Complex		
	August Complex		

The data used for this analysis were from:

- **VIIRS:** The Visible Infrared Imaging Radiometer Suite (VIIRS) data is a crucial tool for fire detection and monitoring across the globe. Operating aboard NASA's Suomi National Polar-orbiting Partnership (NPP) satellite and NOAA's Joint Polar Satellite System (JPSS) satellites, VIIRS provides valuable insights into the dynamics of wildfires, aiding in early detection, assessment, and management efforts. VIIRS is particularly well-suited for forest fire monitoring due to several key characteristics:
  - **High Spatial Resolution:** VIIRS offers moderate-to-high spatial resolution imagery, with some bands providing details as fine as 375 metres. This level of detail allows for the precise identification and mapping of fire-affected areas within forests.
  - **Wide Spectral Coverage:** VIIRS collects data across a broad range of spectral bands, including both visible and infrared wavelengths. This comprehensive spectral coverage enables the detection of fires through their thermal signatures, even in heavily forested areas where smoke and cloud cover may obscure visible flames.
  - **Day/Night Observations:** VIIRS's Day/Night Band (DNB) allows for fire detection not only during daylight hours but also at night. This capability is crucial for continuously monitoring fire activity, as many wildfires may intensify during nighttime when traditional optical sensors might be ineffective.
  - **Frequent Overpasses:** VIIRS operates aboard polar-orbiting satellites, which provide global coverage multiple times per day. This frequent revisit time ensures that fires can be detected and monitored at regular intervals, facilitating timely response efforts.
- **Surface fuel types:** Layers developed by Technosylva following the Scott & Burgan (2005) methodology describing the type of vegetation, their structure and also aridity (e.g., dry, wet, etc) that finally comprises a fuel type code. Surface fuels layers at 30-m spatial resolution were selected for the beginning of the fire season every year.
- **NIFC Perimeters:** The datasets of historical fire perimeters provided by the National Interagency Fire Center (NIFC) offer a wealth of information on past wildfire incidents across the United States. Here are some key types of information commonly included in these datasets:
  - **Fire Perimeter Geometry:** The datasets delineate the spatial extent of each wildfire by providing the perimeter geometry, often in the form of polygons or line segments.

- **Fire Name and Incident ID:** Each wildfire perimeter is typically associated with a unique identifier, typically the fire agency Code, the year and the incident code.
  - **Fire Start and End Dates:** The datasets include information on the date and time when each wildfire started and ended (*FireInitialDate* and *FireContainmentDate*). This temporal information is essential for understanding the duration of fire events and analysing temporal patterns in wildfire occurrences.
  - **Fire Size:** The datasets provide metrics on the size of each wildfire, such as the total area burned or the length of the fire perimeter.
  - **Geospatial Attributes:** In addition to the fire perimeter geometry, the datasets may include geospatial attributes such as elevation, land cover type, and terrain characteristics for the fire-affected areas. These attributes provide contextual information that can be used for spatial analysis and modelling of wildfire behaviour.
  - **Metadata and Documentation:** The datasets often come with metadata and documentation that provide additional details about the data sources, processing methods, and quality assurance procedures. This documentation helps users understand the dataset's limitations, assumptions, and best practices for interpretation and analysis.
  - Overall, the datasets of historical fire perimeters provided by NIFC offer comprehensive information on past wildfire incidents, facilitating research, management, and decision-making related to wildfire risk assessment, mitigation, and response.
- **Satellite imagery Landsat:** Landsat, a program managed jointly by NASA and the United States Geological Survey (USGS), offers satellite imagery renowned for its contribution to Earth observation. With a temporal resolution allowing for frequent revisits every 16 days, Landsat captures changes over time with precision. Its spatial resolution, of 30 metres (ranging from 15 to 60 metres), delivers detailed views of Earth's surface. Landsat imagery typically comprises multispectral data across several bands, including visible, near-infrared, and thermal wavelengths, facilitating diverse applications like land cover classification, agricultural monitoring, urban planning, and environmental assessment. For this study, Landsat8 OLI/TIR was used since it provides data from 2013 until now.

### 3.1.1. Relationships between FRP, surface fuel types and burn severity

This section analyses the relationships between the energy released by the fire, expressed as FRP (Fire Radiative Power) in relation to the type of fuels found in the forest fires and the severity of burning. In this way, the aim is to find patterns in which higher energy releases are associated with higher fuel loads (woodland or shrubland) and higher burn severities.

To understand the thresholds and values of the energy released by the fire, animated graphs were prepared to assess the FRP values during fire spread and define the energy threshold to use for the analysis (Figure 1). The transitions revealed that  $FRP \geq 75$  megawatts correspond to values associated with a flame front, while lower values correspond to areas where smouldering is present or where the fire has already passed. Therefore, VIIRS points with  $FRP \geq 75$  megawatts were used for the FRP analysis.

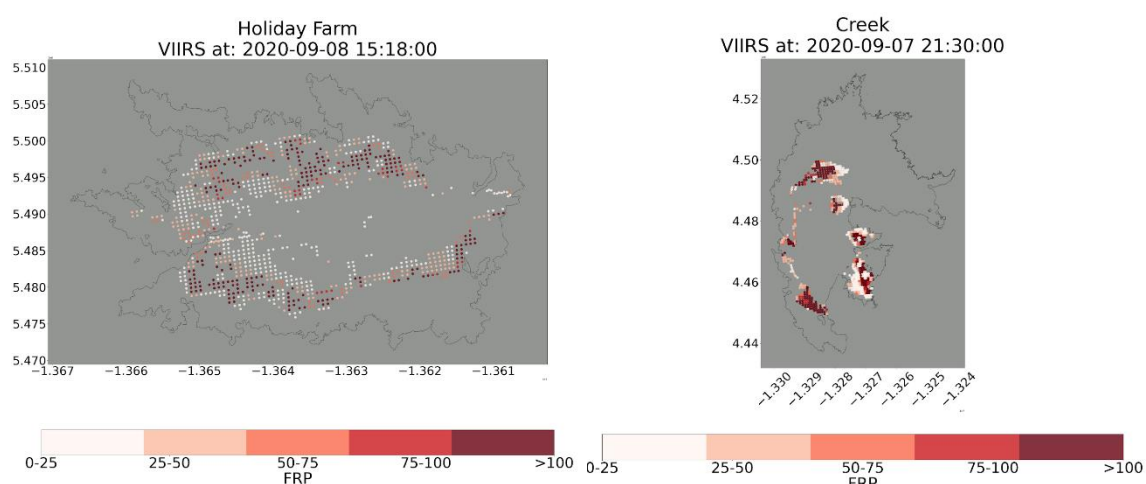


*Figure 1 The animations showed that 75 megawatts was a good threshold to identify the hotspots at the fire front*

The methodology proposed (Figure 2) for this analysis consisted in:

- Collect VIIRS satellite data for each year.
- Filter the data for each perimeter and date of the forest fire.
- Remove FRP outliers (out of the Interquartile Range).
- Extract point data from fuel and severity raster.
  - Remove all the urban/ settlement and water classes.
  - Reclassify the severity from 4 classes (i.e., 4, 5, 6, 7) to two classes: 4 and 5 to Low severity (1); 6 and 7 to High severity (2).
- Plot the data.
  - Bar Plots: They represent the relative importance of the VIIRS hotspots presence within a fuel type in a forest fire. To do this, the number of VIIRS hotspots falling inside a fuel is divided by the count pixels of that fuel in the forest fire. In this way, the representation of the energy is relative to the area of fuels.

- Violin plots: The data distribution of the FRP for each fuel is represented in a graph using density curves and a boxplot. The lines of the boxplot represent the limits of the first and third quantiles.

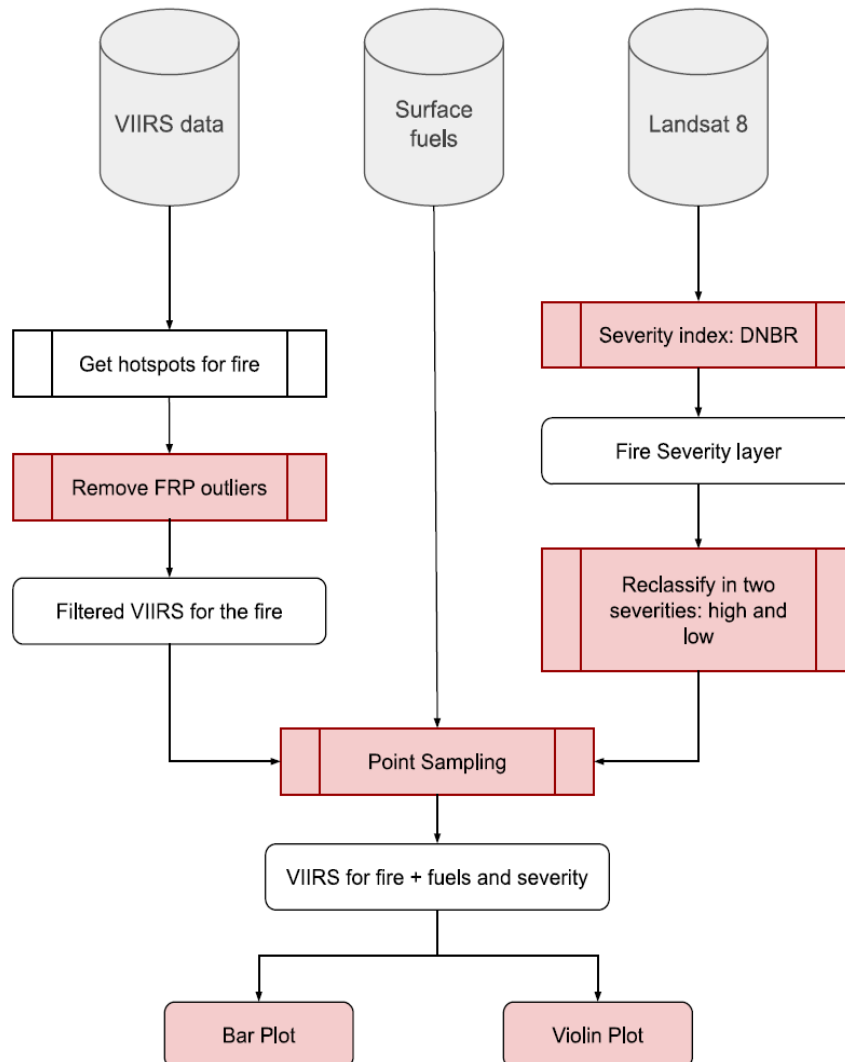


Figure 2 The workflow followed

The graphs were plotted for each forest fire and for all the fires of the year (Figure 3A, 3B and 3C). Two sub graphs were created for interpreting the results. A violin plot showing the energy distribution per fuel and a bar plot showing the representation of the VIIRS point in the fuel of the fire. This is a way to contrast if there are many points in a low represented fuel, or few points in a very represented fuel, which would mean that the fuel is not prone to burning.

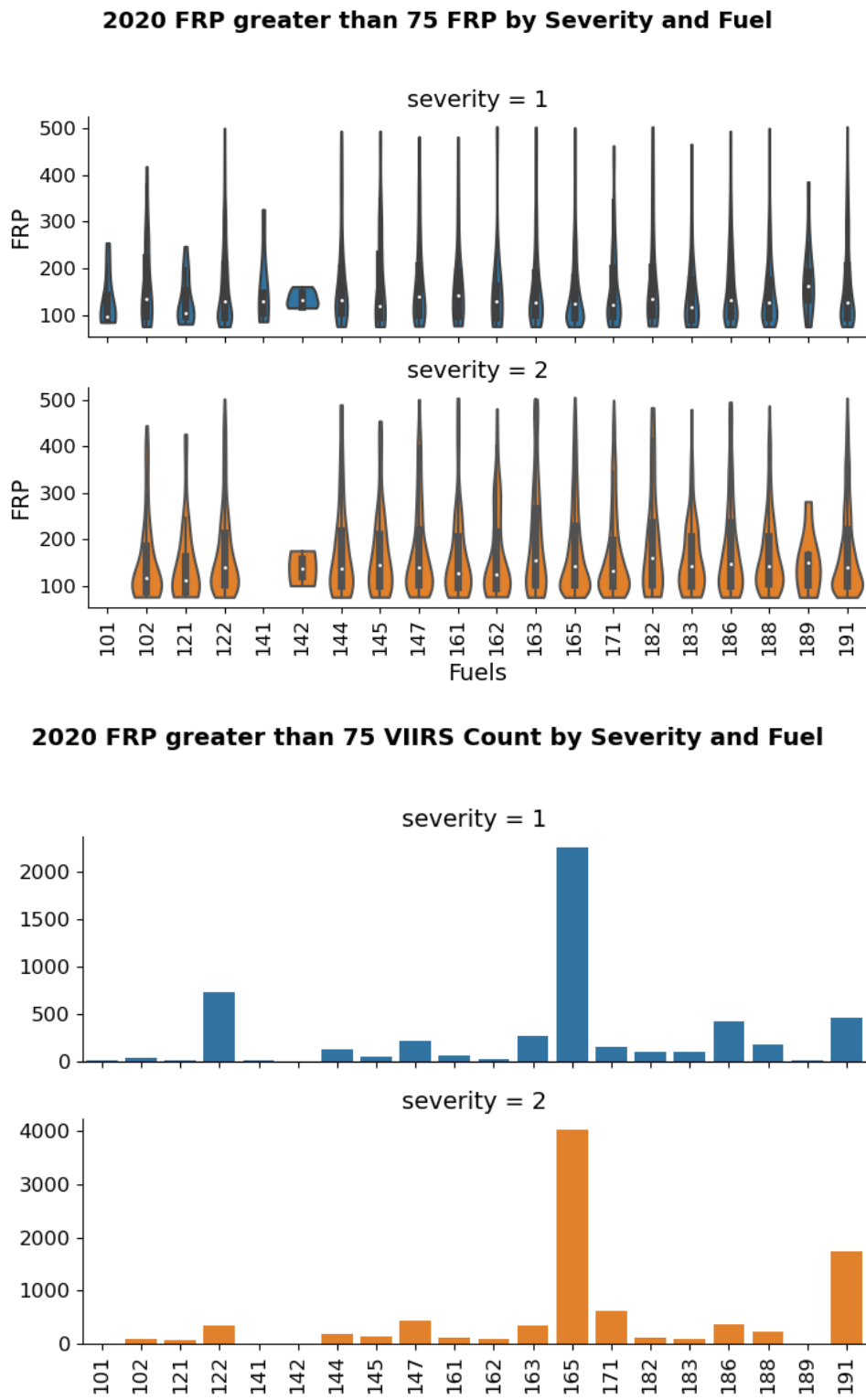


Figure 3A Violin and bar plots for 2020; for the two levels of severity: 1= low and 2 = high. The X axes represent the coded fuels from Scott & Burgan (2005) and the Machine Learning fuels developed by Technosylva

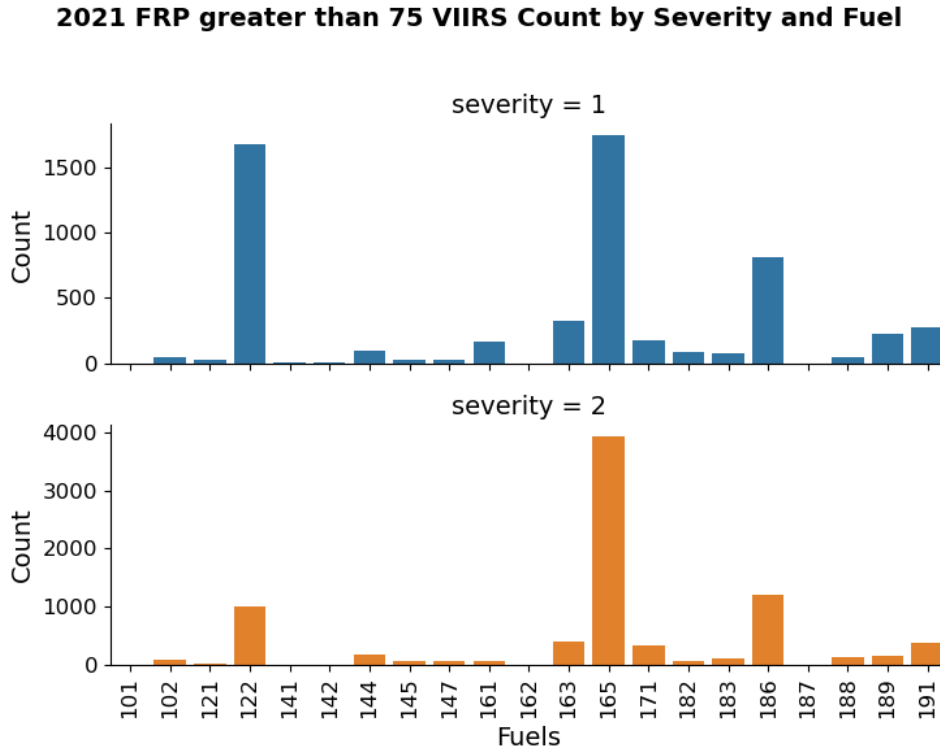
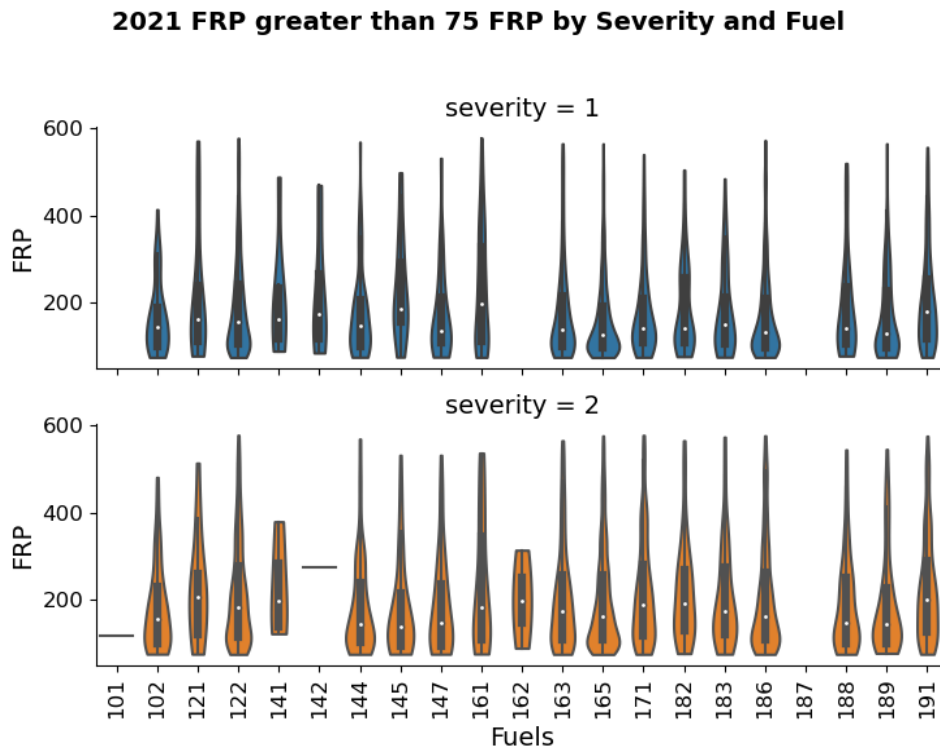
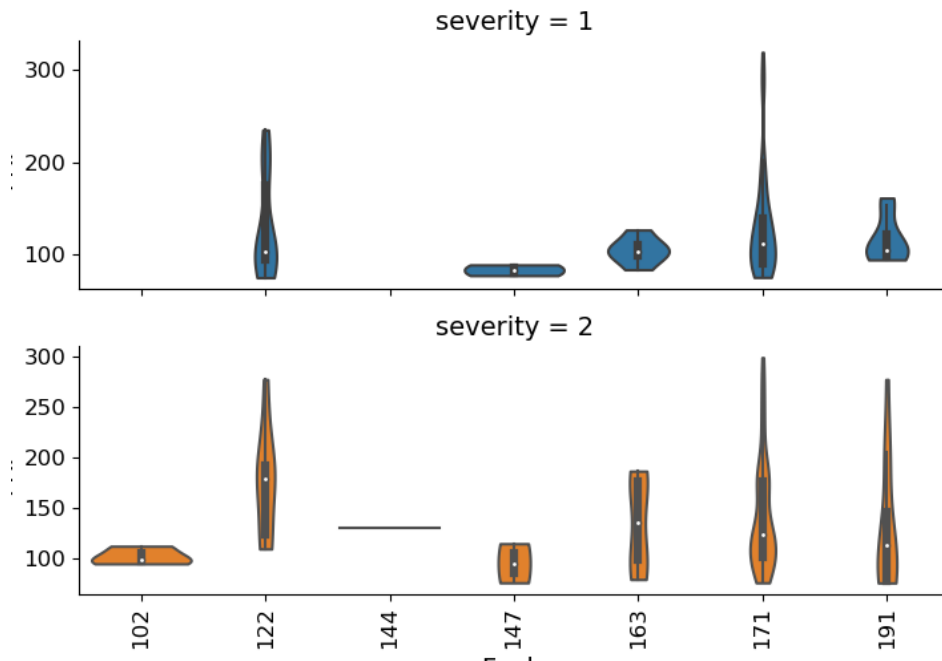


Figure 3B Violin and bar plots for 2021; for the two levels of severity: 1= low and 2 = high. The X axes represent the coded fuels from Scott & Burgan (2005) and the Machine Learning fuels developed by Technosylva

**2022 FRP greater than 75 FRP by Severity and Fuel**



**2022 FRP greater than 75 VIIRS Count by Severity and Fuel**

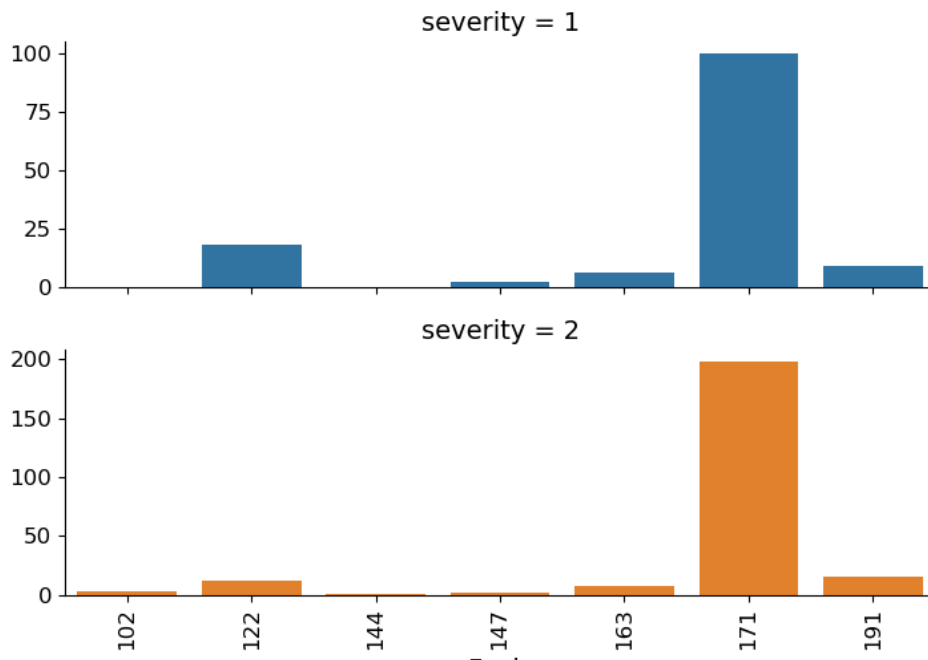
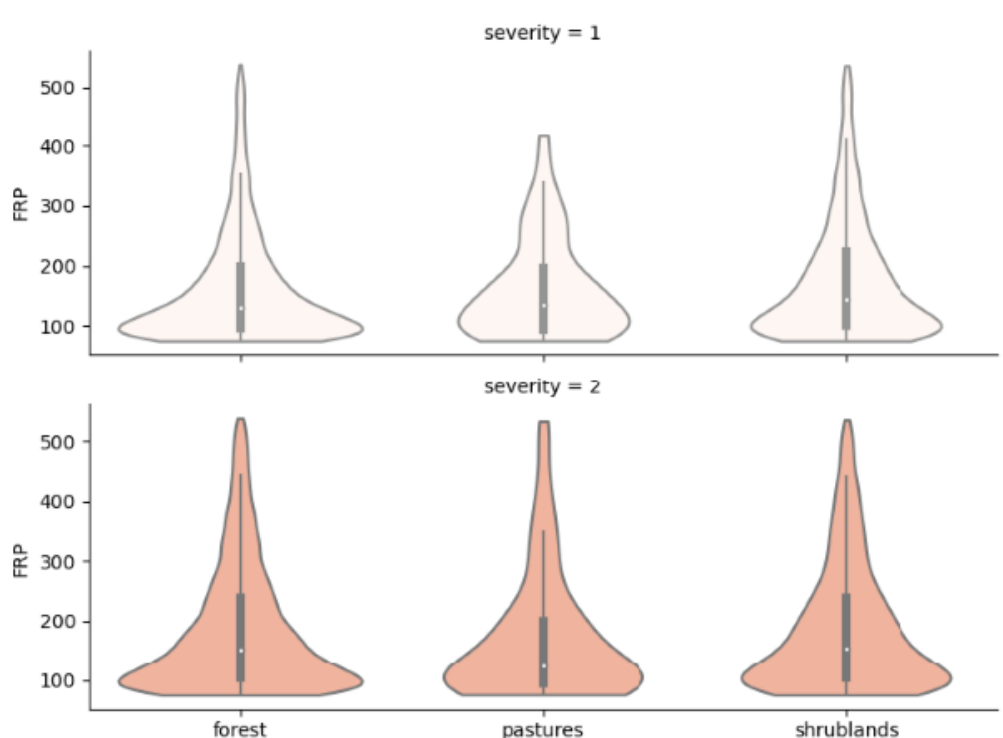


Figure 3C Violin and bar plots for 2022; for the two levels of severity: 1= low and 2 = high. The X axes represent the coded fuels from Scott & Burgan (2005) and the Machine Learning fuels developed by Technosylva

It was difficult to associate higher energies with fuel types since differences are not big enough between groups. Therefore, a coarser analysis was run grouping the fuels into three wider classes (i.e., grasslands-pastures, shrublands and forest) to find clearer differences. The original codes were grouped into the aforementioned categories: grasslands-pastures from 100 to 119, shrublands from 120 to 159 and forest from 160 to 199. Additionally, the 3-year data was summarised under one graph to avoid describing yearly characteristics of the fires (Figure 4).



*Figure 4 Violin plot for FRP above 75% and the three fuel categories (forest, pastures and shrublands) classified by low severity (upper panel) and high severity (lower panel)*

The FRP violin plot divided into severities shows that for severity 1 (low severity), although the median of the distributions is similar, the highest energy release occurs in shrublands, where, in the box plot, it reaches its highest upper limit compared to the other categories. On the other hand, as expected, in severity 2 (high severity), grassland has a lower energy release compared to the forest and shrubland typologies. However, between the latter two categories, there do not seem to be significant differences in the distribution of FRP. Both show a similar boxplot configuration and density curves. The only difference is that the forest type fuels are the most heavily represented in the data set and thus explain the difference in width between the two violin plots between forest and shrubs.

### 3.1.2. FRP vs Weather metrics

In this section, two analyses are proposed using the FRP as a response variable. The objective is to: (1) find for specific weather conditions how FRP distribution is reflected among the fuel models, and (2) find thresholds in atmospheric variables at which changes in the distribution and release of wildfire energy can be observed.

For both analyses, a dataset combining FRP from VIIRS data and environmental variables was prepared including:

- Weather data from weather stations.
  - Temperature in Celsius degrees (°C).
  - Wind speed in km/h.
  - Wind gusts in km/h.
  
- Drought indicators and Fire danger indices historical data from the Copernicus Emergency Management Service (Deprecated 2023-06-14). In this dataset, the following variables can be found:
  - Fire weather index.
  - Build up index.
  - Danger risk.
  - Drought code.
  - Duff moisture code.
  - Initial fire spread index.
  - Fine fuel moisture code.
  - Fire daily severity rating.
  
- Drought indexes from the gridMET datasets were added to the target variables. The drought indexes were the Standardised Precipitation-Evapotranspiration Index (SPEI) for 90 days, the Standardized Precipitation Index (SPI) for 90 days, and the Evaporative Demand Drought Index (EDDI) for 90 days. Each data point was associated with the drought indexes spatially and temporally.

As in the previous section, VIIRS data with FRP values greater than 75 were selected. In addition, to remove outliers from the analysis, only the FRP values falling inside the interquartile range were kept (and above 75). Therefore, first quartile (Q1) \*1.5 to third quartile (Q3) \*1.5. In addition, values below 75 within Q1 and Q3 were discarded.

Next, for the first analysis (finding FRP distribution in fuels under target weather conditions) to represent the environmental conditions in fire events, two groups of variables were proposed following expert criteria:

- The first, all VIIRS points showing burning affection (severity 1 and 2; or conversely, the categories different to 0) and relative humidity below than 60%.

- The second one comprises the areas with high severity burning affections (severity 2), presenting wind speed over 25 km/h, relative humidity below 20%, and temperature over 30 °C.

The outputs were aggregated for each fuel types according to Scott & Burgan (2005) codes (Figure 5), which are as follows:

- Grass: 101 and 102.
- Grass-Shrub: 121 and 122.
- Shrub: 141, 142, 144, 145 and 147.
- Timber Understory: 161, 162, 163 and 165.
- Timber Understory (Dynamic, 2022 update): 171.
- Timber Litter: 182, 183, 186, 188 and 189.
- Timber Litter (Dynamic, 2022 update): 191.

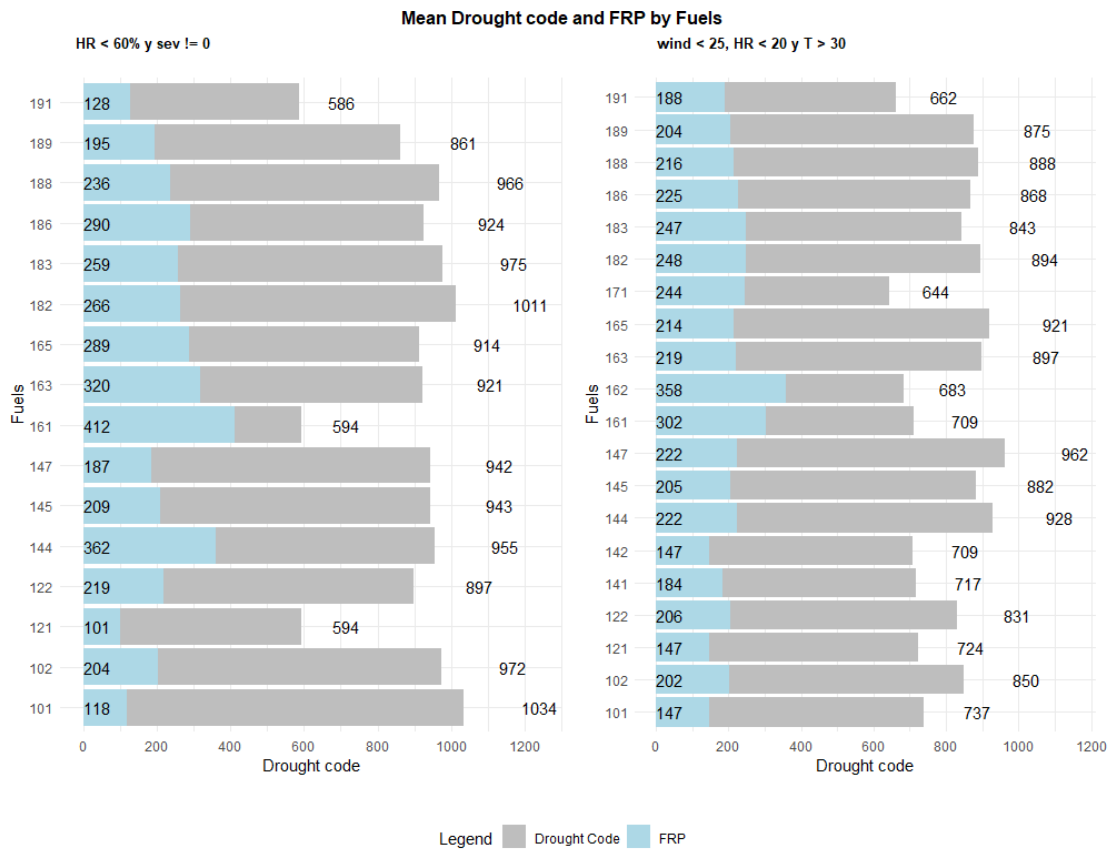


Figure 5 Bars plot for mean Drought Code and FRP for each fuel code, separated by relative humidity <60 % and low severity (left panel); and by wind speed <25 km/h, relative humidity <20 %, temperature > 30° C and high severity (right panel)

In the second analysis, the objective is to understand how energy release behaves against weather variables and find thresholds that indicate shifts in the FRP values. For that, every variable was reclassified in intervals, and the mean FRP was calculated for each group. Moreover, error was calculated for each group to understand the variability within each group. The results were plotted in bar charts with error bars. The variables analysed were:

- **Wind gust (km/h).** The gust speed was reclassified in 4 groups: 0-20, 20-25, 25-35, and >35 km/h. The main finding here is that FRP seems to present higher values when wind gusts exceed **25 km/h** (Figure 6).

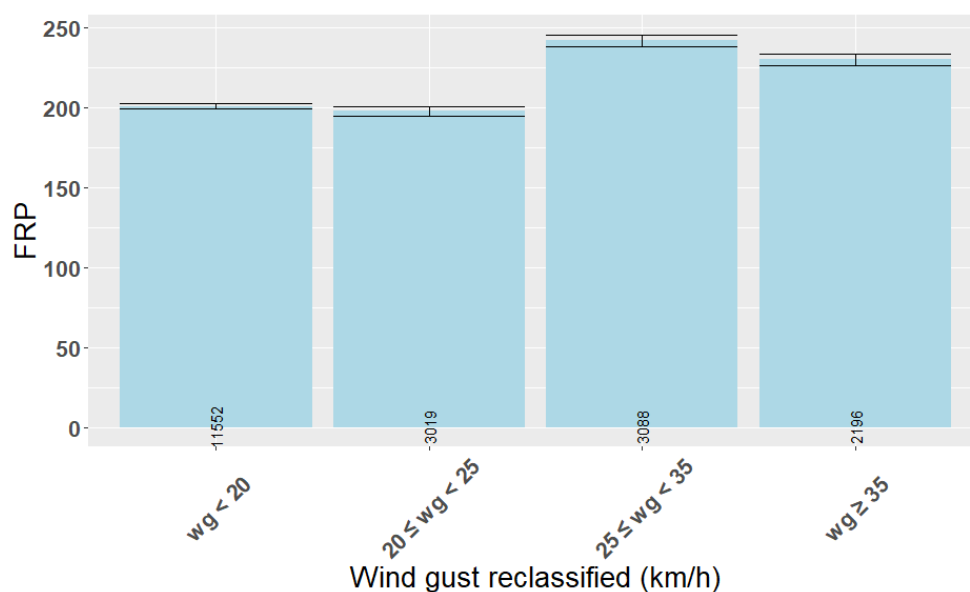


Figure 6 Bars plot for mean FRP in each wind gust speed threshold (error bars represent the mean's uncertainty)

- **Wind speed (km/h):** As in wind gusts FRP values increase with higher wind speeds. Most of the values concentrate on the lower wind speed. However, FRP values present a significant increase as of 20 km/h (Figure 7).

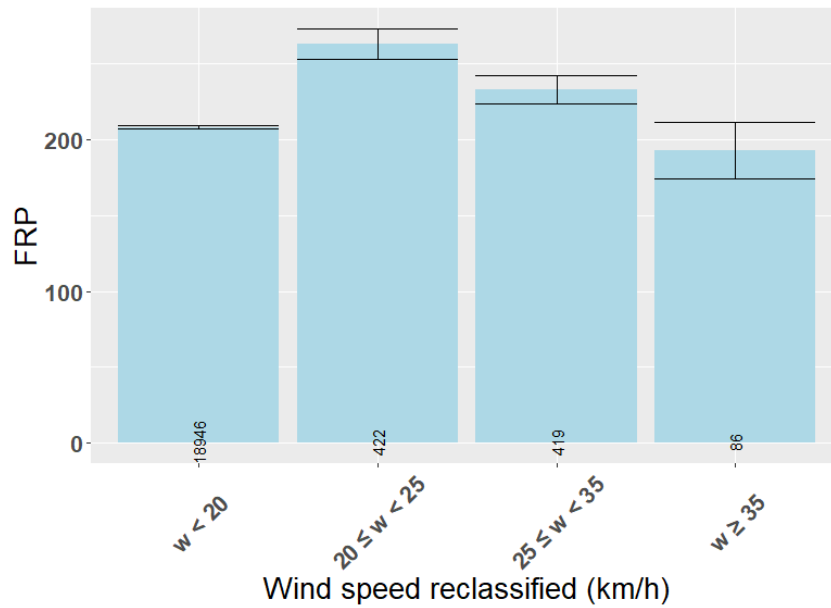


Figure 7 Bars plot for mean FRP in each wind speed threshold (error bars represent the mean's uncertainty)

- Relative humidity (%):** The relative humidity was reclassified in 6 groups: <10, 10-20, 20-30, 30-40, 40-60, and >60%. In this analysis the FRP increases as the relative humidity lowers. However, no threshold could be inferred from Figure 8.

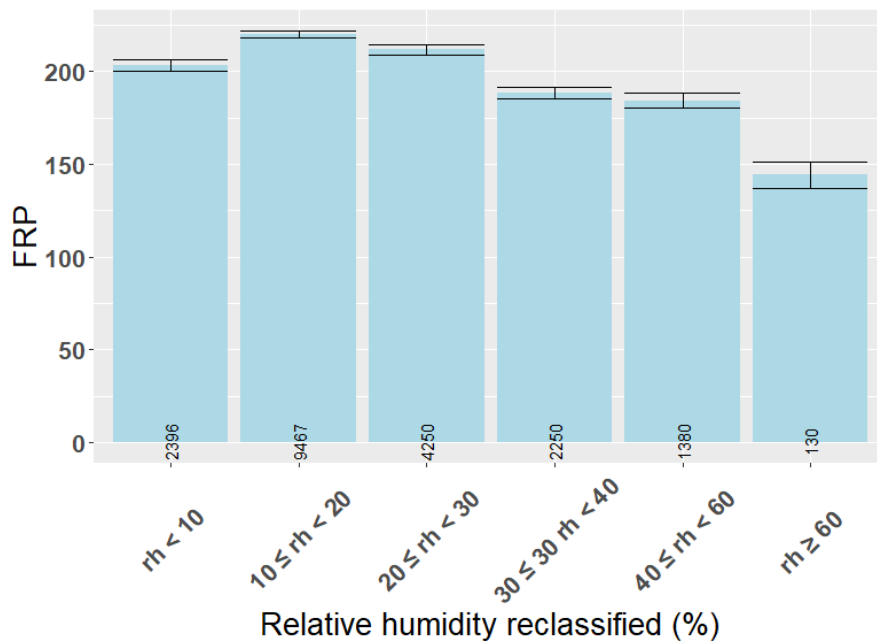


Figure 8 Bars plot for mean FRP in each relative humidity threshold (error bars represent the mean's uncertainty)

- **Temperature (°C):** The temperature was reclassified in 4 groups: <20, 20-30, 30-35, and >35°C. Although FRP tends to increase with temperature a threshold was not identified using this method for temperature (Figure 9).

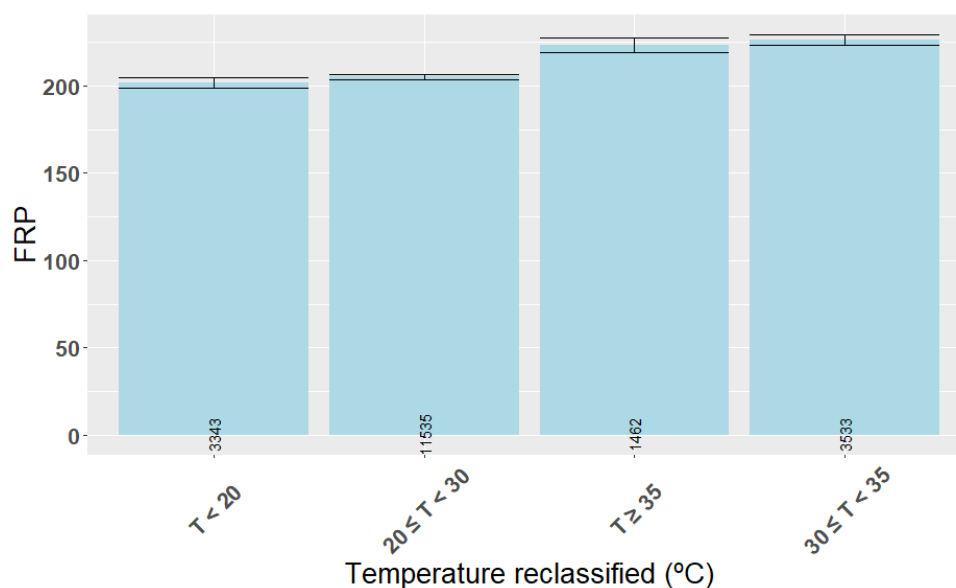


Figure 9 Bars plot for mean FRP in each temperature threshold (error bars represent the mean's uncertainty)

### 3.2. ROS vs Weather metrics (Wind Speed) and Atmospheric instability metrics (Lifted Index, Convective Flag)

The goal of this chapter is to understand the relationship between the weather/ atmospheric instability variables and the rate of spread. The hypothesis is that the highest ROS should occur under higher wind speeds and unstable atmospheric conditions. Atmospheric instability was represented by the lifted index measured at different atmosphere levels (500 hPa and 600 hPa). We use the FireGuards dataset from 2020 to 2023, only available in California, which records the progression of fire events and provides both fire perimeters and rate of spread. Figure 10 shows an example of one of these fires with its corresponding FireGuards polygons and rate of spread vectors. Then, for each vector, weather data was associated using as a reference the coordinates and time when the fire spread started.

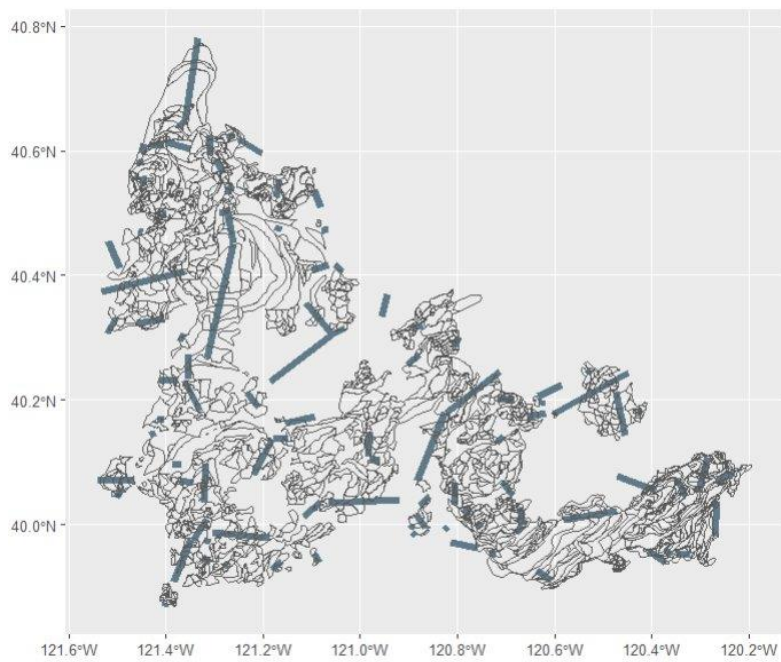


Figure 10 Spatial distribution of FireGuard polygons and fire spread vectors for the Dixie fire (July 2021)

The values extracted for the vectors were aggregated in categories and plotted. The first metric evaluated was wind speed. Figure 11 shows a positive trend between the fire spread and wind speed dropping towards the higher wind classes.

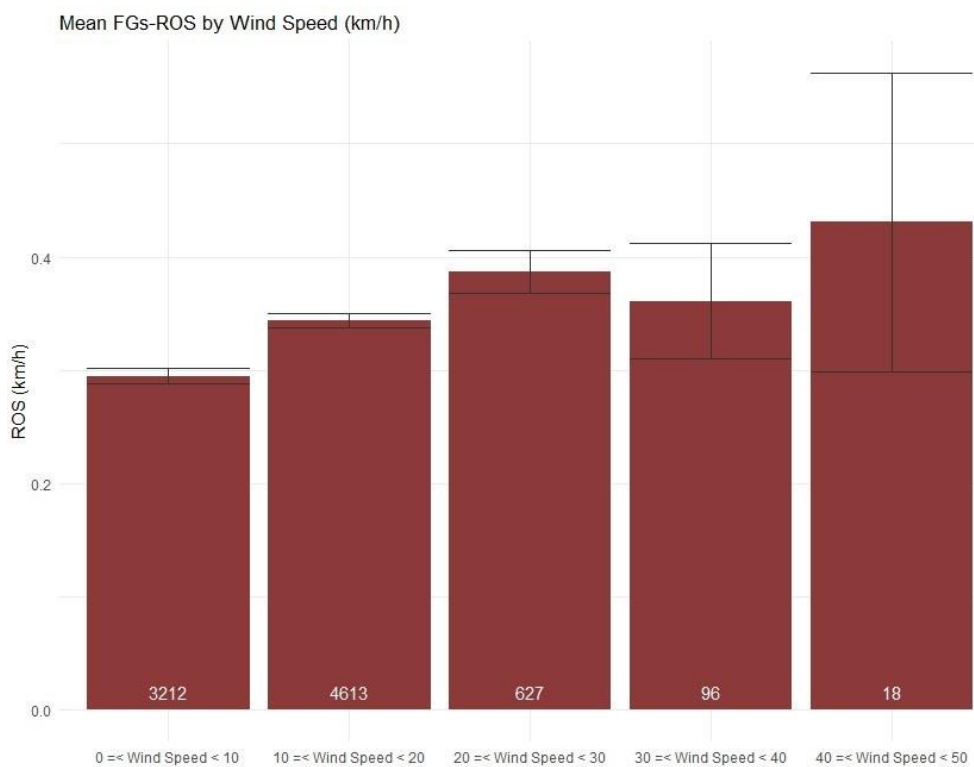


Figure 11 Bars plot for mean ROS derived from FireGuards polygons for each wind speed threshold

Regarding the instability metrics (Figures 11, 12, and 13), the rate of spread increases under unstable atmospheric conditions. Out of all the lifted index metrics, the values at 500 hPa High-Resolution Rapid Refresh (HRRR) show the fastest fire propagations. Another of the findings in the analysis is that using Lifted index values at 500 hectopascals (Figures 12 and 13), higher instability values were obtained, where the highest fire spreads are found at values between -6 and -2, compared to those extracted at 600 hPa (Figure 14), where the highest ROS values appear when the lifted index is between -2 and 0.

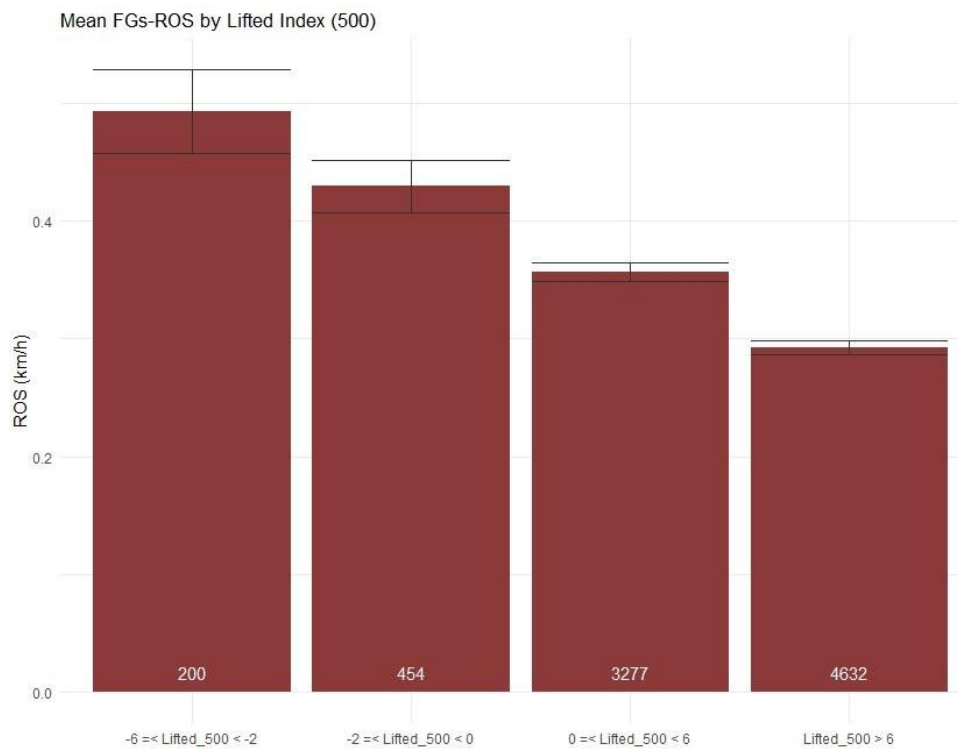


Figure 12 Bars plot for mean ROS derived from FireGuards polygons for each lifted index threshold (at 500 hPa)

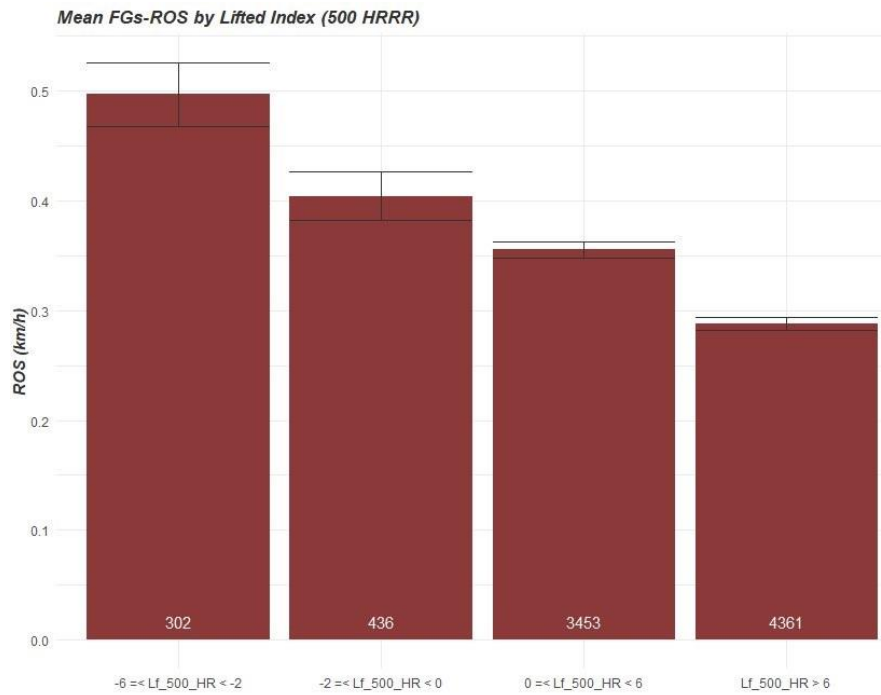


Figure 13 Bars plot for mean ROS derived from FireGuards polygons for each lifted index threshold (at 500 hPa by HRRR model)

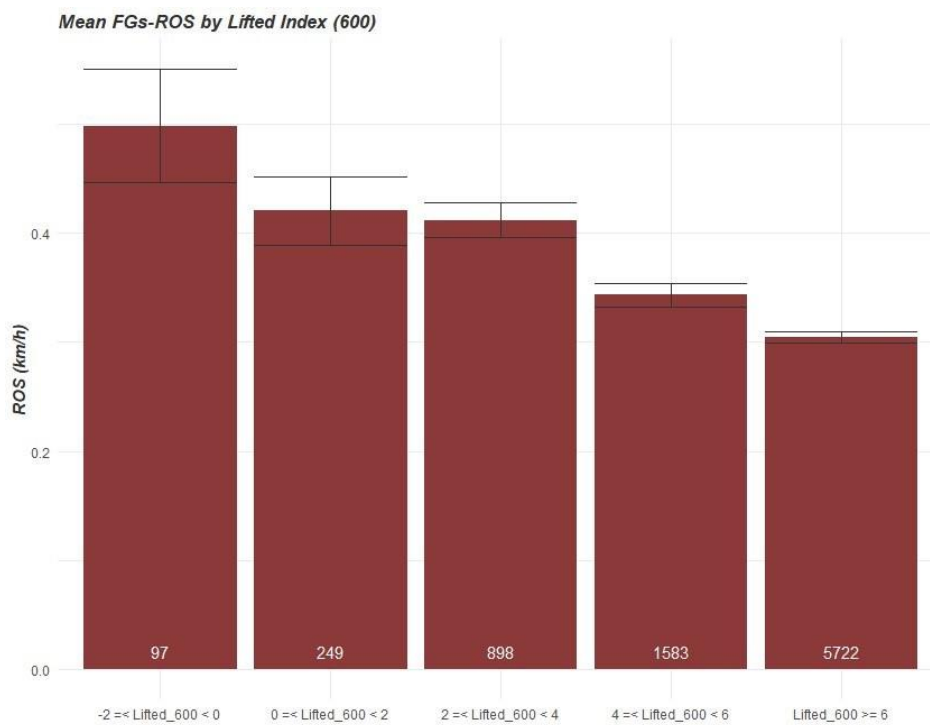


Figure 14 Bars plot for mean ROS derived from FireGuards polygons for each lifted index threshold (at 600 hPa)

Another element to be analysed was the relationship between ROS and convection in forest fires. For this evaluation, the variable Convective Flag was used as an indicator of atmospheric convection. This parameter is of special interest because it can help to categorise convective events from wind events, since it quantifies the ratio of surface fire potential to convective fire potential to flag environmental conditions suitable for pyrocumulonimbus development. Its values usually range from 1 to 10, where any value below 8 is considered as instable conditions. Figure 15 shows how the fastest vectors are those that are in convective conditions (Convective flag < 8). Although no continuous trend of ROS growth was identified as the convective flag decreases under unstable conditions (Convective flag < 8), significant differences in ROS were found comparing unstable (Convective flag < 8) and stable atmospheric conditions (Convective flag > 8).

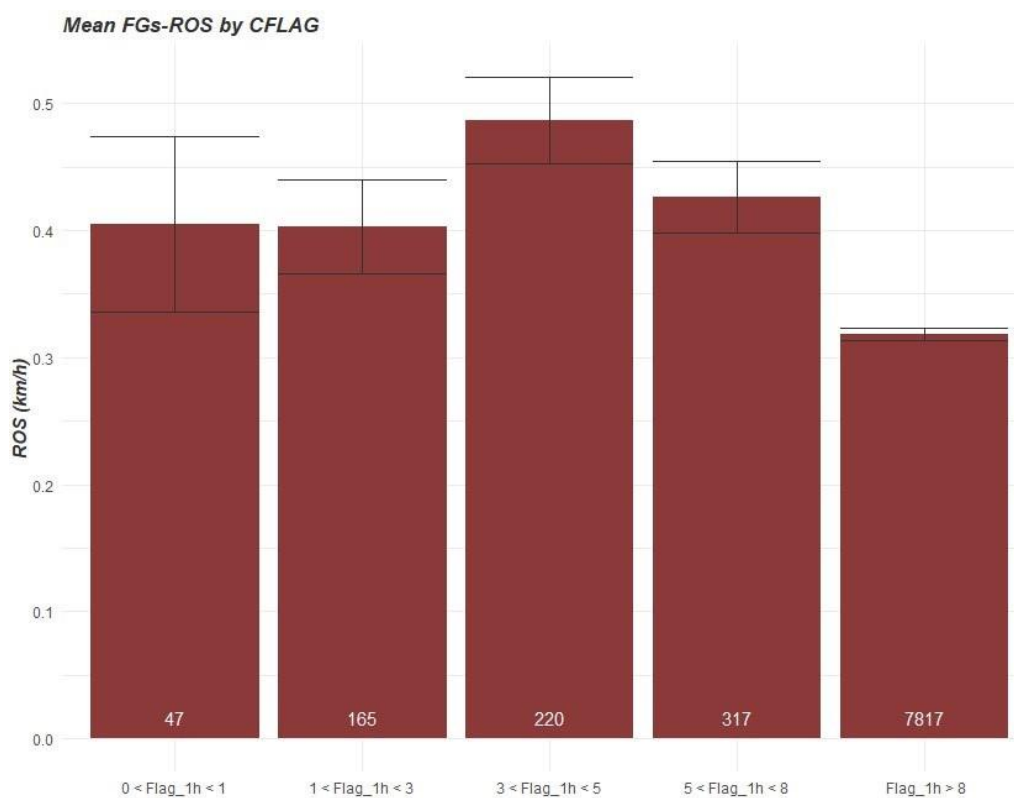


Figure 15 Bars plot for mean ROS derived from FireGuards polygons for each 1-h convective flag threshold

### 3.3. Pyrocumulous presence

The objective of this analysis was to explore the correlation between Pyrocumulous presence and the occurrence of convective fire behaviour, especially in Extreme Wildfire Events. For this purpose, the **Pyrocumulonimbus Firepower Threshold** (PFT) index was selected, which was developed in Australia to identify deep pyro convective events (Tory and Kepert, 2021). PFT attempts to objectively calculate the height of the condensation level for a given plume and environment, and it ultimately predicts the energy release, in Gigawatts (GW), that the fire must produce in order to generate Pyrocumulonimbus (PyroCb). In that sense, lower PFT correlates with a more unstable atmosphere and an increased likelihood of PyroCb formation.

However, there are some limitations associated with validating the PFT because reliable observations of fire radiative power during these intense fires are not available. Sensor saturation and cloud interference do not allow satellite derived FRP to be leveraged to validate the PFT. In order to solve these caveats, a validation effort led to an approach called the **PFT Flag** or **Convective Flag**. Tory and Kepert (2021) observed that PyroCb does not occur when the PFT flag is greater than 5, therefore lower values indicate more unstable conditions.

A total of 15 wildfires were employed as locations to validate Convective flag performance (Table 2), the majority of them in California and one in Oregon, representing unique convective profiles. The ratio was evaluated not only to assess true atmospheric instability, but also to objectively evaluate the potential instability and the likelihood of a fire releasing that potential instability.

*Table 2 List of the 15 fire incidents employed for PFT Flag validation*

<b>Incident Name</b>	<b>Type of validation</b>
<b>Antelope</b>	Fire life
<b>Beckwourth</b>	Fire life
<b>Bootleg</b>	Fire life
<b>Caldor</b>	Fire life
<b>Lava</b>	Fire life
<b>McFarland</b>	Fire life
<b>Monument</b>	Fire life
<b>Salt</b>	Fire life
<b>Tamarack</b>	Fire life
<b>Tenant</b>	Fire life
<b>Valley</b>	Fire life
<b>CZU</b>	Fire initiation
<b>SCU</b>	Fire initiation
<b>LNU</b>	Fire initiation
<b>Loyalton</b>	Fire initiation

The main results of Convective Flag performance pointed out that PyroCb does not occur when the value is over 5, so this is consistent with Tory's observations. Therefore, the index is useful in predicting extreme convective fire behaviour. Additionally, a fair predictive skill with less intense convective fire behaviour was observed (e.g., pyrocumulous (PyroCu)). Ultimately, four breakpoints in the Convective Flag values were proposed: at 1, 2-4, 5 and 6-8 to enable the index to forecast convective fire behaviour of both PyroCu and PyroCb. In the case of the probability of detection of all convective fire behaviour, both PyroCu and PyroCb (Figure 16), there is no bias when the Flag is 5, and the probability of detection stabilises when the Flag is 8. In the case of Success Ratio, this is maximised when Flag is 1 (i.e., fewest false alarms) and the Critical Success Index is stabilised for all categories when Flag is between 2 and 4.

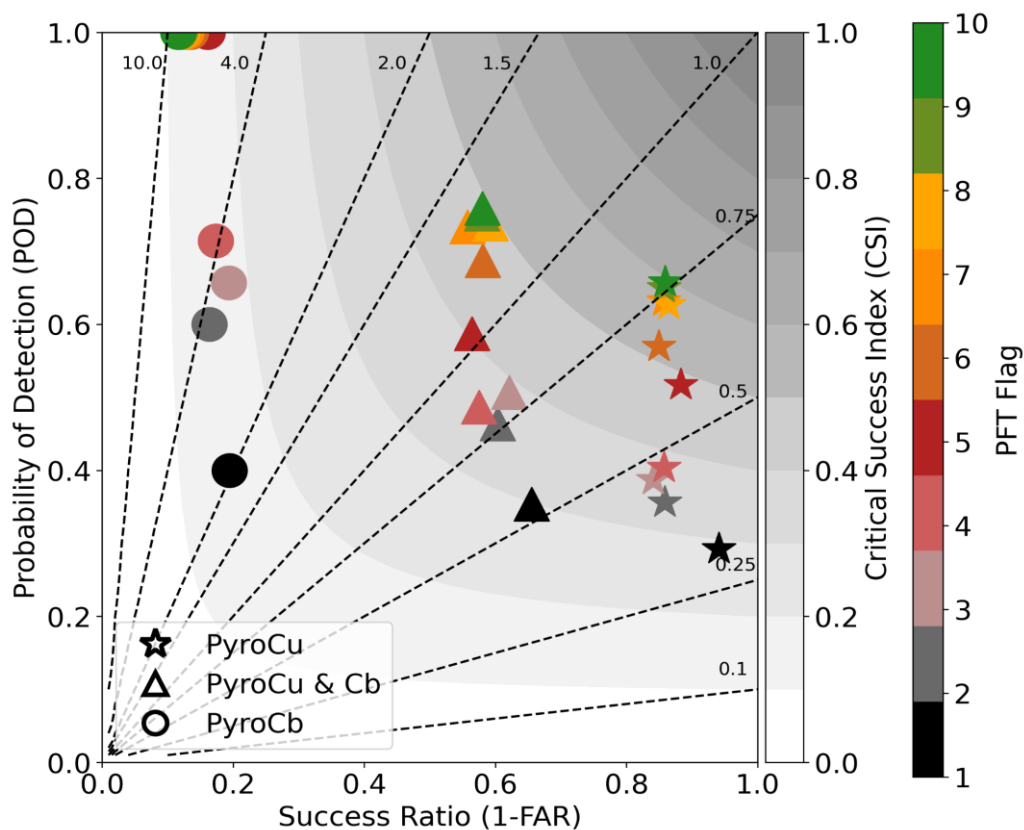


Figure 16 Relationship between Probability of Detection (POD), Success Ratio (SR) and Critical Success Index (CSI) for each PFT Flag category in the Pyrocumulous, Pyrocumulonimbus and Pyrocumulous & Pyrocumulonimbus presence

As a summary, after evaluating the index's ability in the Western US to predict pyrocumulous and pyrocumulonimbus presence, coining it the Convective Flag to improve operational adoption efforts was proposed. Lower values indicate a more unstable environment and yield the fewest false alarms in the 15 events sampled. Further, the probability of detection improved with acceptable increases in false alarms when the index remained below eight. The Convective Flag should be further evaluated across different fire regimes to assess its predictive skill in identifying the potential for

convective fire behaviour (i.e., moist pyroconvection such as pyrocumulous or pyrocumulonimbus).

### 3.4. Methodology transference to European scenario

This analysis has been run for the United States of America, showing relationships between fire spread and convective phenomena. However, these analyses have relied on data provided by private entities (weather data) or public data that are not readily accessible to the public (FireGuards). Therefore, it is necessary to define a methodology with public access data that can be carried out in Europe.

The main constraint is to find a dataset equivalent to FireGuard that provides ground truth fire rate of spread values. This information can be achieved in some European countries' environment offices or fire institutions, but since Europe is composed of a large number of members (51), the data collection and standardisation among datasets would greatly hinder the progress of the analysis.

To overcome these difficulties, the methodology proposed uses VIIRS as a database given its high temporal and spatial resolution and its global availability. The main goal is to derive isochrones and rates of spread vectors from VIIRS points. For that, fire activity data points are grouped in 12-hour intervals (theoretical revisit period) to avoid having periods of fake or repeated data that can produce abnormally high ROS values.

Once the VIIRS are clustered in 12-hour intervals, the alpha shape of each timestep is calculated to derive isochrones polygons. From every temporal consecutive polygon, spread vectors are drawn, calculating the rate of spread by dividing the distance between polygons by 12h. Finally, for the ROS vectors dataset, the fastest vectors are extracted for each timestep and fire, to obtain the main spread direction of the fire.

On the other hand, it is necessary to find a replacement for the dataset describing the weather and atmospheric conditions (stability and winds). For that purpose, although spatially coarser (~27.75 km), [ERA5 offered a wide range of products](#) at global scale with hourly resolution and global cover (Hersbach et al., 2023). For the analysis the following variables were selected:

1. 10 metres U-component of neutral wind. Units in m/s.
2. 10 metres V-component of neutral wind. Units in m/s.
3. Convective Available Potential Energy (CAPE). As cited in the ERA5 dataset description, CAPE "is an indication of the instability (or stability) of the atmosphere and can be used to assess the potential for the development of convection". Units in J/kg.
4. Instantaneous 10 metres wind gusts. Units in m/s.

Both data for ERA5 and VIIRS data were downloaded from 2012 to 2023 for the Iberian Peninsula. For each main fire propagation vector calculated, all the variables were extracted and ROS was compared to the variables, in order to look for patterns in the ROS behaviour, mainly looking for relationships between fire spread and convection processes.

CAPE values lower than 1000 J/kg represent weak instability (i.e. stability conditions) and more than 1000 J/kg moderate instability. In this case, there are less fire spread propagation vectors under a stable atmosphere. However, those vectors in moderate and high instability doubled the ROS under stable conditions (Figure 17).

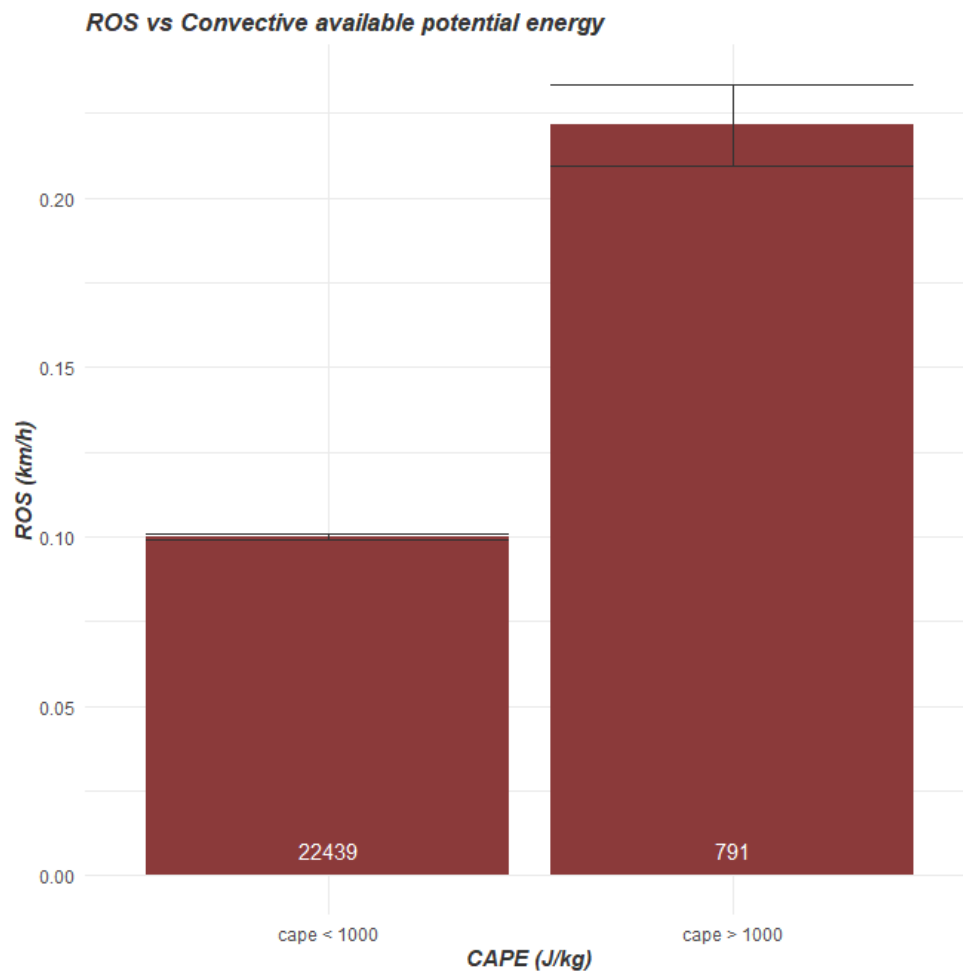


*Figure 17 Bars plot for mean ROS derived from fire propagation vectors and the Convective available potential energy (CAPE) threshold*

One of the clearest relations found were those between ROS and instantaneous wind gusts (Figure 18). An exponential increase of the mean ROS when wind gusts are greater is detected. Ranging from average ROS of 0.075 km/h within wind gusts below 15 km/h to mean ROS over 0.175 km/h for wind gusts over 60 km/h.

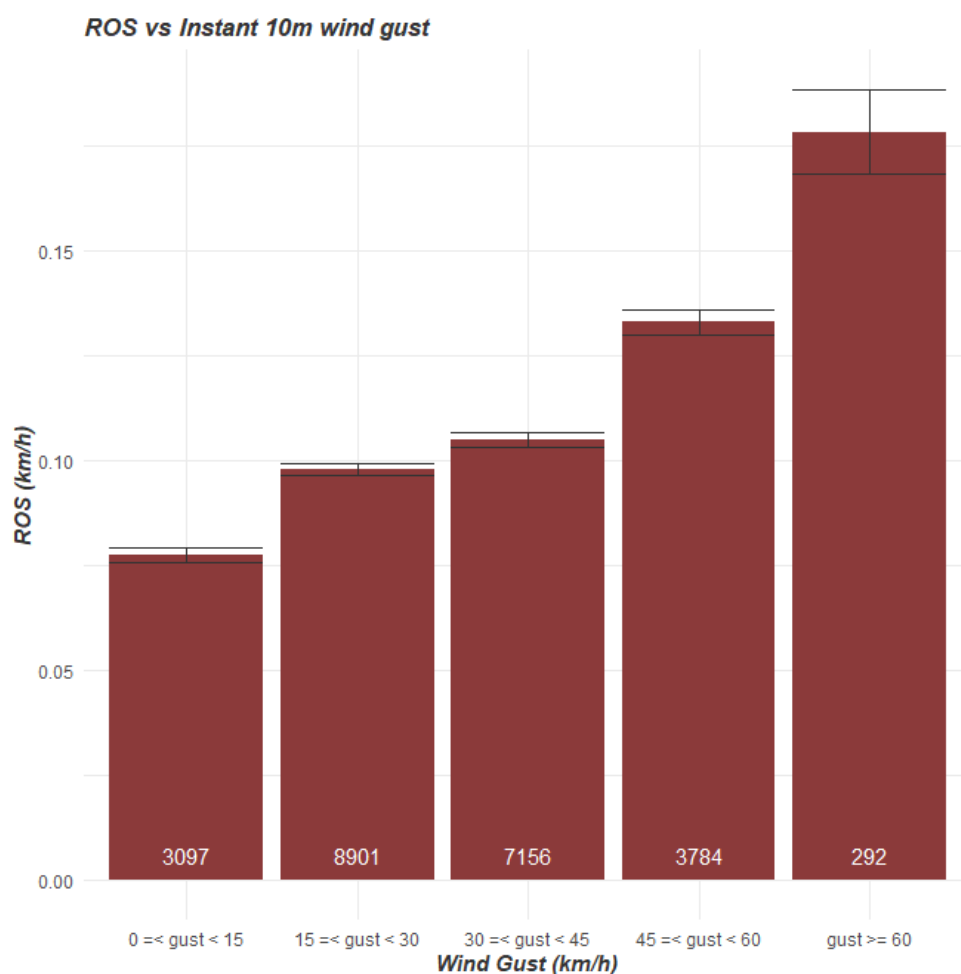


*Figure 18 Bars plot for mean ROS derived from fire propagation vectors and different instantaneous wind gust (at 10m height) thresholds*

Finally, for the case of neutral wind speed, again an increase trend is shown in Figure 19. However, at the highest wind speeds (between 30 and 40 km/h), a lower mean ROS (0.125 km/h) was found compared with the previous threshold (i.e., from 20 to 30 km/h) with an average ROS more than 0.15 km/h. This behaviour could simply be explained due to the fact that the analysed fire propagation vectors usually do not reach that highest wind speeds (depending on the wind patterns recorded, types of fuels and their moisture content, among other factors).

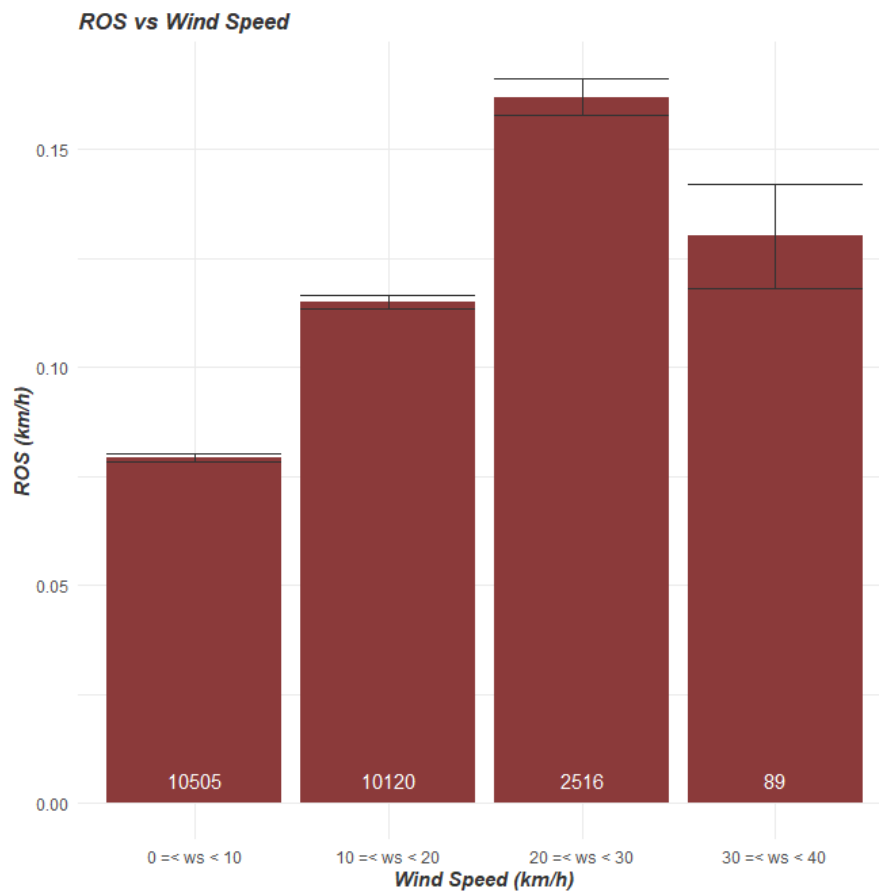


Figure 19 Bars plot for mean ROS derived from fire propagation vectors and different wind speed (at 10m height) thresholds

## 4. Implementation

### 4.1. FireSim updated model including lifted index

FireSim web has implemented an internal fire behaviour adjustment factor in the wildfire simulation code to adapt the fire propagation to Extreme Wildfire Events conditions. The above-mentioned change was finally materialised into a ROS adjustment factor model based on the Lifted Index, which is obtained from Spire's forecast weather data grids. It contributes to better simulating and estimating the behaviour of the EWEs. This adjustment is implemented for both deterministic and probabilistic simulations.

For **deterministic fire simulations**, this adjustment equation was implemented when Lifted index  $\leq 0$  °C and dead FMC  $< 6\%$ , following the equation:

$$ROS_{adj} = 1.15 + \text{abs}(\text{Lifted}) * 0.15$$

where *ROS<sub>adj</sub>* is the Rate of Spread adjustment to be used in the fire simulation, and Lifted corresponds to Lifted index, which is the temperature difference between the environment  $T_e(p)$  and an air parcel lifted adiabatically  $T_p(p)$  at a given pressure height in the troposphere (lowest layer where most weather occurs) of the atmosphere, usually 500 hPa (mb).

For **probabilistic simulations**, it would be necessary to employ the range of variation of this adjustment.

Regarding the implementation of the FireSim code, the necessary values for dead fuel moisture content and the lifted index will be sourced from the nearest measurement to the fire's ignition point. Once the rate of spread (ROS) adjustment is determined, the simulation will proceed with a final ROS calculated as  $ROS_{adj} * ROS$ , thereby enhancing the fire's potential. This ROS adjustment will be the same for all fuels, including the WUI urban areas.

### 4.2. Validation of wildfire simulations under unstable conditions

In this analysis, the objective was to individually compare the rate of spread registered by FireGuards polygons versus the ROS derived by the simulated perimeters (conducted under simulations in the Technosylva's Wildfire Analyst - WFA). For this, a total of 24 wildfires that occurred in California from 2020 to 2022 (Table 3) were employed in unstable atmospheric conditions (i.e., lifted value  $< 0$ ). It is known that under these convective circumstances, wildfires commonly originate pyrocumulous and pyrocumulonimbus. This type of phenomenon is usually very local and originates its own meteorology closely linked to a virulent fire behaviour. This means rapid and

momentaneous wind speed increases (especially intense gusty winds) together with erratic wind behaviour (sudden direction changes) and thus, unexpected fire propagation.

The aim was to validate both sources (FireGuard's and WFA's ROS) in these critical fire convective events due to their high impact both in the environment and more specifically in the humans (infrastructures, residences or lives).

The steps used for this analysis were:

- 1) Filtered those FireGuard polygons with ROS over 10 km/h and with an available lifted value below 0 (i.e., representing unstable atmospheric conditions).
- 2) Match the resulting FireGuard polygons with IRWIN's wildfire database by the closest ignition time.
- 3) Select the last or furthest FireGuard date-time.
- 4) Measure the distance from the ignition point (the first FireGuard recorded) to the furthest point of the last FireGuard and divide by the fire duration in hours.
- 5) Conduct individual simulations for each fire incident, taking into consideration the fire duration in hours.
- 6) Measure the distance from the ignition point to the furthest point of the simulated perimeter and divide by the duration in hours.

*Table 3 List of the 24 fire incidents with lifted value < 0 selected for the fire simulation (FS) and FireGuard (FG) ROS comparison. Note that ROS (FS) values are calculated using the ROS adjustment for convective scenarios*

Incident Name	FireSim Duration (h)	FG date/time	ROS (FS) km/h	ROS (FG) km/h
Markan Ridge	30	08/19/2020 21:19:00	0.10	0.09
Del Puerto	25	08/17/2020 16:32:00	0.52	0.55
Holser	24	08/18/2020 14:13:00	0.13	0.11
Barnes	33	09/09/2022 00:15:00	0.09	0.24
Fairview	4	09/05/2022 19:39:00	1.17	0.84
W-5 Cold Springs	34	08/19/2020 19:55:00	0.53	0.19
Bobcat	41	09/08/2020 05:11:00	0.25	0.21
Mosquito	62	09/09/2022 08:30:00	0.17	0.23

<b>Carmel</b>	26	08/19/2020 14:56:00	0.27	0.21
<b>Radford</b>	34	09/06/2022 23:26:00	0.11	0.11
<b>Rancho Chaparral</b>	8	08/28/2021 20:31:00	0.43	0.40
<b>Yeti</b>	20	07/30/2022 16:58:00	0.07	0.10
<b>McCash</b>	10	08/02/2021 04:43:00	0.03	0.28
<b>Sheep</b>	56	08/19/2020 19:53:00	0.13	0.16
<b>Dexter</b>	80	07/15/2021 18:09:00	0.16	0.04
<b>Oak</b>	59	08/07/2022 17:03:00	0.06	0.05
<b>Antelope</b>	81	08/04/2021 19:34:00	0.11	0.26
<b>Doe</b>	61	08/18/2020 21:56:00	0.11	0.10
<b>Windy</b>	78	09/12/2021 23:53:00	0.09	0.03
<b>River</b>	67	08/18/2020 21:36:00	0.17	0.20
<b>Colony KNP Complex</b>	84	09/13/2021 19:37:00	0.07	0.02
<b>Caldor</b>	76	08/17/2021 22:48:00	0.09	0.27
<b>Mcfarland</b>	73	08/01/2021 19:46:00	0.05	0.07
<b>Ammon</b>	82	08/08/2022 12:44:00	0.09	0.05

In general terms, the ROS values are quite similar between those registered by the FireGuard polygons and the simulated ones (Figure 20). However, in some fire incidents, simulations tend to overestimate the expected rate of spread. These are the cases of W-5 Cold Springs and Dexter wildfires with a double simulated ROS value (0.53 km/h and 0.16 km/h, respectively) than the reported FireGuard's ROS (0.19 km/h and 0.04 km/h, respectively). On the contrary, other wildfires registered a higher ROS from FireGuards than their simulated perimeters, pointing out that in some cases, WFA simulations underestimate the rate of spread in some sectors of the fire front. Specifically, Barnes and McCash fires, with simulated ROS values of 0.09 km/h and 0.03 km/h, respectively; compared to the FireGuards ROS values of 0.24 km/h and 0.28 km/h, respectively.

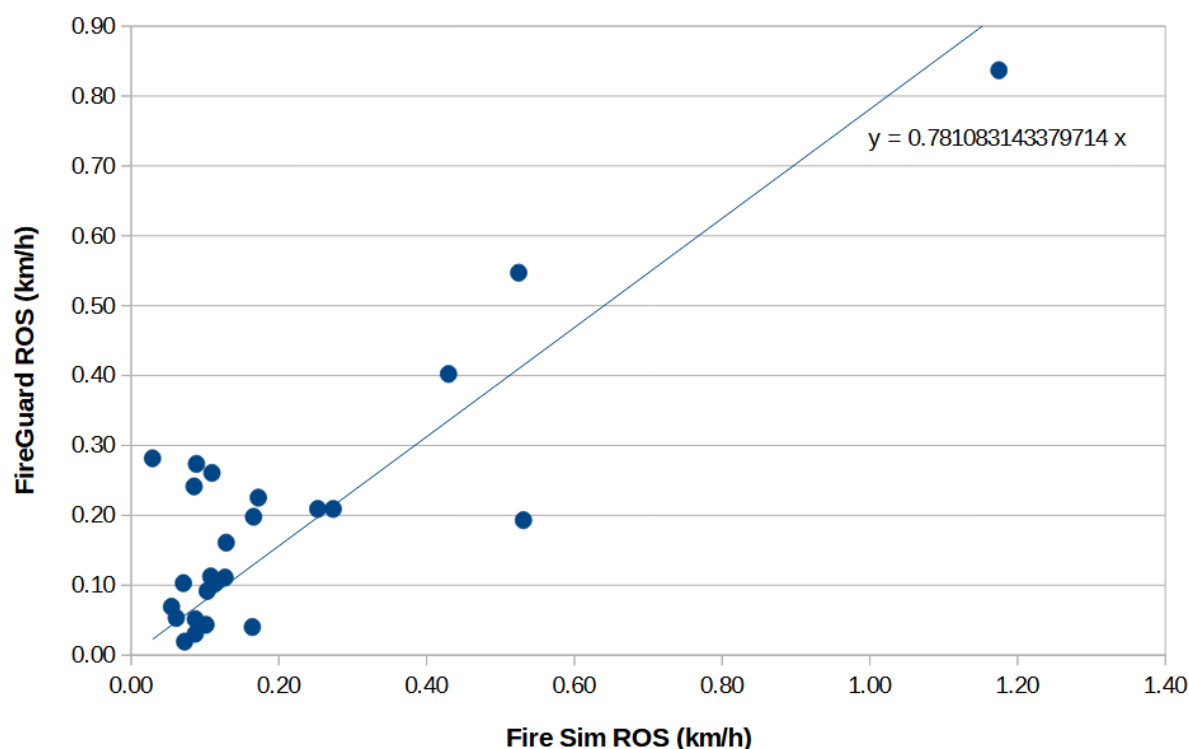


Figure 20 Scatter plot for ROS derived from the last/furthest FireGuard polygon versus ROS derived from the simulated perimeter in the same direction of FG vector in WFA

It can be concluded that WFA simulated ROS matched in general to a great extent with the FireGuards' ROS values, despite the fact that the ROS patterns are more difficult to model and predict under unstable conditions. Note that this method proved how the model was able to predict the average ROS in moderate-long fire runs. However, it must be recognised that abrupt changes in ROS during short periods across the duration of these fire runs may not have been predicted.

### 4.3. FireRisk and FireSim apps implementation

In the next sections, the FireRisk and FireSim applications implementation process within the FIRE-RES project are described. For the case of the FireRisk module, its main outputs are different FireRisk metrics at territorial level across the extent of the four Living Labs (LLs). The major purpose is to provide the end user with the zones of the territory that present higher risk for the corresponding metrics with the aim of supporting forest fire mitigation planning.

Regarding the FireSim module, it is based on the operational simulation capabilities of Wildfire Analyst (WFA) from Tecnosylva, where the aim is to provide near real-time forest fire behaviour modelling and spread prediction through deterministic and also stochastic modelling approaches, providing forest fire behaviour results and pyroconvective

indicators in a few minutes. Ultimately allowing a rapid understanding of the potential impacts and consequences of fire on the population and buildings.

Finally, the addition of high-resolution weather was implemented by means of Weather Research and Forecasting (WRF) data to the FIRE-RES Integrative System Platform (ISP). This data includes current HR weather data as well as HR weather forecast data. The latter is foreseen to be visualised by the users for their analysis and to be consumed by other modules such as the TSYLVA FireRisk assessment and the FireSim.

#### 4.3.1. Living labs description and scenarios data

The four Living labs were defined by different areas of interest. For the case of Portugal LL, only the north half of the country was considered, previously agreed with the corresponding LL leaders. For Catalonia and the domain of the Netherlands' LLs, both coincide with administrative boundaries of the autonomous community and national borders, respectively. Regarding the German domain of the Netherlands-Germany LL, only North Rhine Westphalia and Lower Saxony states were considered. This was decided by the LL leaders. Finally, for the Gran Canary Island LL, only the island territory was covered. It is important to note that these LLs' boundaries were settled in the following FireRisk and FireSim process implementation.

Regarding the scenarios' preparation, for the cases of the LLs where some of the data was not available, it has been possible to find an alternative source of information by making use of public sources of data or by making use of data that has been created by other partners in the WP5. An example of the latter has been the detection of the lack of existence of a vegetation fuel models map for the German LL areas (North Rhine Westphalia and Lower Saxony). This has been addressed by making use of the FIRE-RES fuel maps for these areas that were created and made available by the Università degli Studi di Padova (UNIPD) (see Kutchartt et al. 2024) in the WP5 in task 5.6.

Another example has been the lack of suitable geospatial population and building data in the Portuguese, Catalonia and Gran Canary Island LLs. For those cases it has been possible to make use of publicly available data sources, such as Worldpop for the population data and, Microsoft buildings and OpenStreetMap's open data sources, for obtaining the necessary buildings data.

The preparation process of Geographic Information System (GIS) scenarios data was conducted for the four LLs and included the inputs detailed in the following subsections (i.e., from 4.3.1.1. to 4.3.1.4.).

#### 4.3.1.1. Portugal Living Lab

- **Fuels.** Fuel data was obtained from Fernandes et al. (2009) fuels adapted to Scott and Burgan and Technosylva scenario Spain version 3 (at 30 m spatial resolution).
- **Buildings.** Retrieved from the combination of OpenStreetMap in Portugal and Technosylva scenario Spain version 3.
- **Population.** Obtained from the open spatial demographic dataset WorldPop.
- **Canopies.** Calculated from Technosylva scenario Spain version 3 and value 0 in Portugal area.
- **Digital Elevation Model.** Obtained from Technosylva scenario Spain version 3.
- **Terrain Difficulty Index.**

#### 4.3.1.2. Catalonia Living Lab

- **Fuels.** In this case, this layer included also canopy data. All these inputs were retrieved from the public PREVINCAT repository at 20 m of spatial resolution which was derived from LiDAR data 2016.
- **Buildings.** Obtained from Technosylva scenario Spain version 3.
- **Population.** Retrieved from 2020 WorldPop Global Project Population Dataset (open access).
- **Digital Elevation Model.** It was retrieved from the PREVINCAT repository at 20 m of spatial resolution.
- **Terrain Difficulty Index.**

#### 4.3.1.3. Netherlands-Germany Living Lab

- **Fuels.** The final fuel layer is a combination from the general fuel map created in the FIRE-RES project for Germany regions and Netherlands scenario version 8 (originally at 30-m spatial resolution). In the case of Netherland, original fuels were converted to equivalent types to Scott and Burgan classification. The Netherlands fuel data was obtained from *Nederlands Instituut Publieke Veiligheid* (NIPV). It also included canopy information derived from the FIRE-RES project (see Kutchartt et al. In Press).
- **Buildings.** Centroids were extracted from Netherlands scenario version 8 for the Netherlands area and OpenStreetMap for Germany boundary regions.
- **Population.** Provided by the Netherlands-Germany partner.
- **Terrain Difficulty Index.** For its confection the starting scenario contained Scott and Burgan fuels for Germany boundaries regions and Netherlands fuels adaptation.

#### 4.3.1.4. Gran Canaria Island Living Lab

- **Fuels.** This information was obtained from Cabildo of Gran Canaria institution.
- **Buildings.** The data source employed was the Cabildo of Gran Canaria.
- **Population.** Same data source employed for buildings.
- **Terrain Difficulty Index.** This layer was the same employed in the Gran Canaria scenario version 7.

#### 4.3.2. Living labs meteorology data

##### 4.3.2.1. Weather Research and Forecasting grid setup

The FireSim environment allows employing both weather forecasts and constant weather. For the case of weather forecast data, this has been downscaled employing the Global Forecast System (GFS) and Weather Research and Forecasting (WRF), which is being generated by Technosylva Inc. using the PANGEA High-Performance Computer (HPC). One of the goals was to show daily weather forecasts in each LL, apart from being inputs for the FireRisk and FireSim simulators. The WRF domains downscale GFS's 27 km grid via a nesting approach, resulting in high-resolution grids (1-2 km horizontal resolution) for the innermost domains of each LL and a forecast horizon of four days (i.e., 96 hours ahead).

- **Portugal Living Lab.** Three nested domains (18 km, 6 km, and 2 km) were established, with the innermost domain having a 2 km resolution across the Living Lab (Figure 21). The default 2 km resolution was employed, and again complex terrain was avoided at domain boundaries where possible.

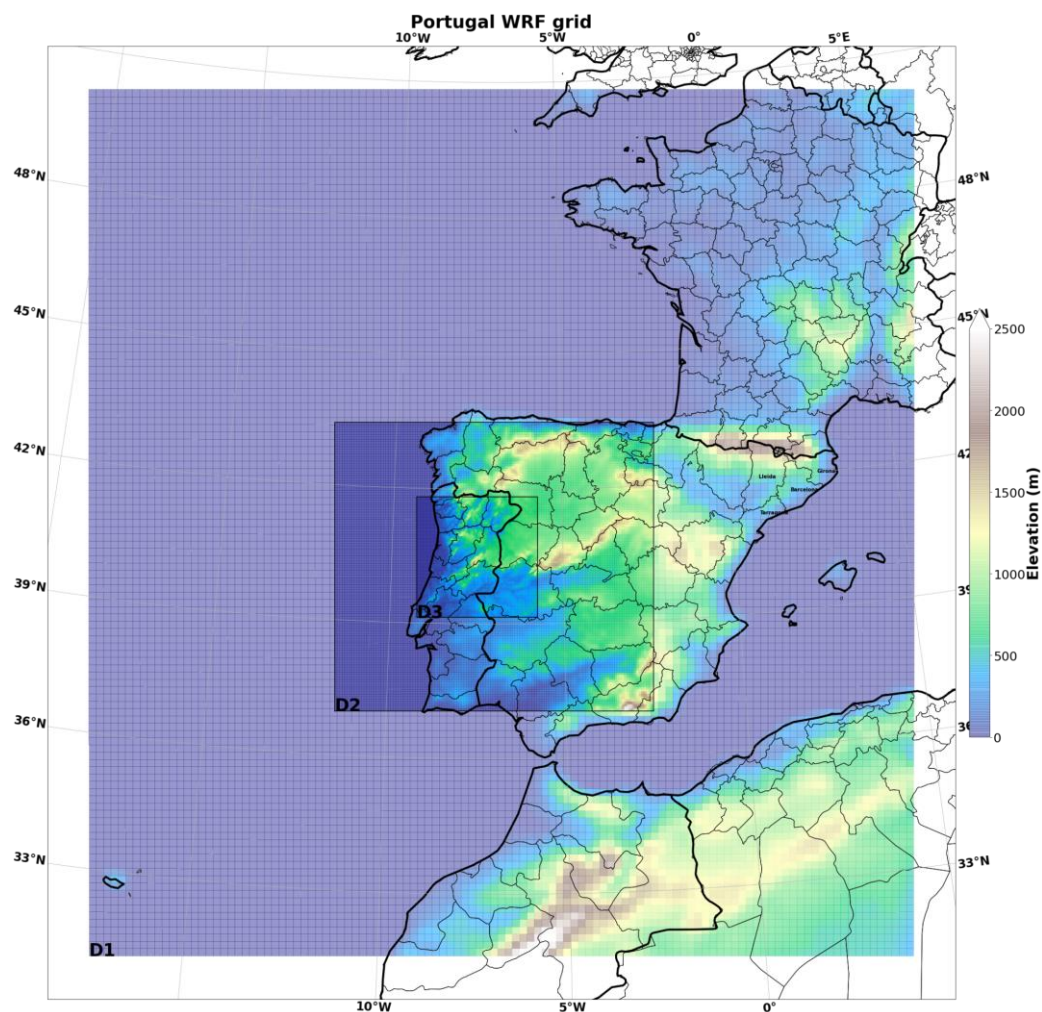


Figure 21 Portugal WRF grids of 18, 6 and 2 km spatial resolution

- Catalonia (Spain) Living Lab.** Three nested domains (18 km, 6 km, and 2 km) were established, with the innermost domain having a 2 km resolution across the Living Lab (Figure 22). The innermost domain strategically encapsulated the entire Pyrenees range to avoid complex terrain near the domain boundary and capture most of the Ebro basin, which has significant fire weather implications for Catalonia. The finest resolution of 2 km was selected based on the findings of Cao & Fovell (2016), which identified 2 km as the optimal horizontal resolution for capturing critical fire weather patterns.

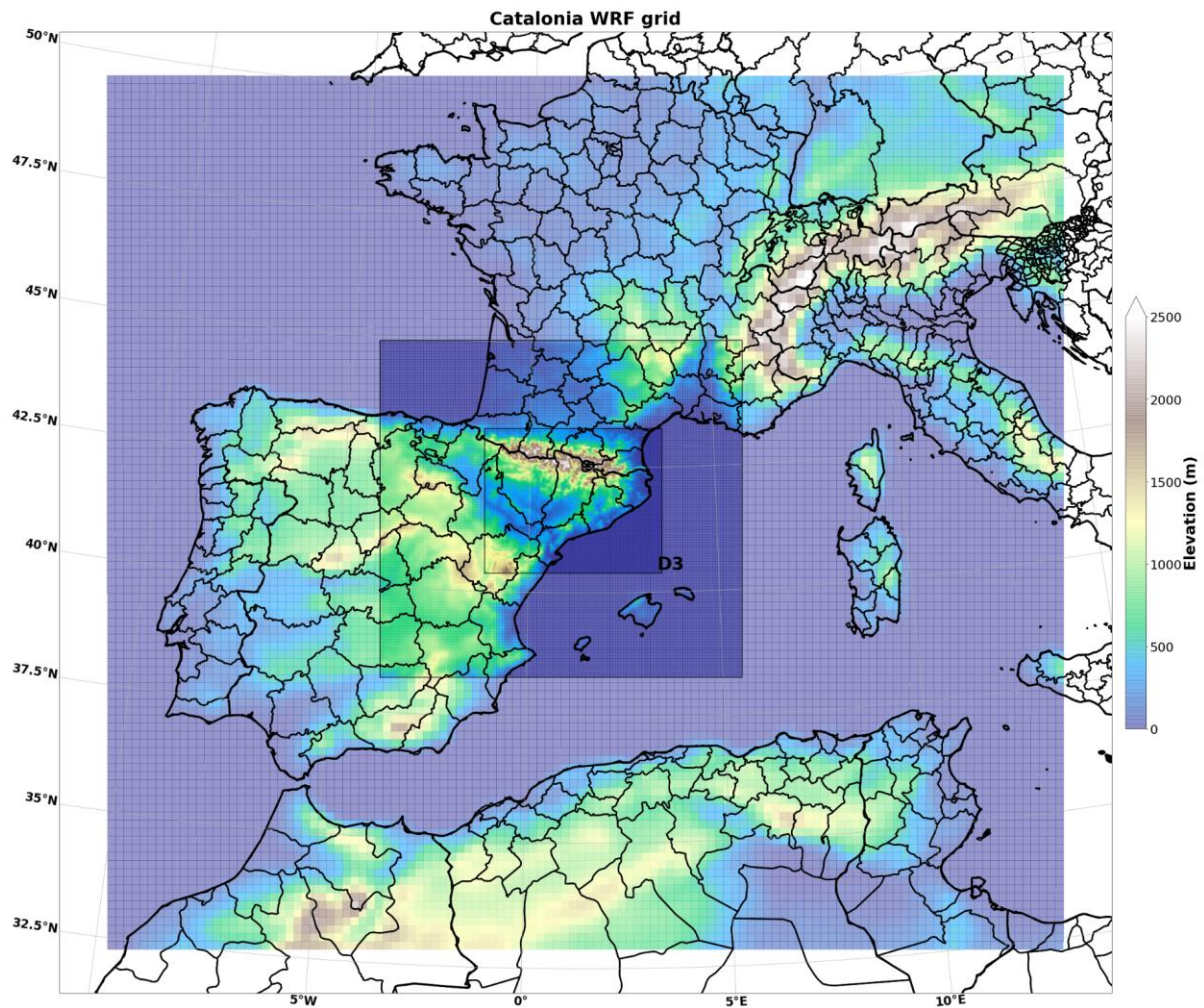


Figure 22 Catalonia WRF grids of 18, 6 and 2 km spatial resolution

- Netherlands - Germany Living Lab.** Three nested domains (18 km, 6 km, and 2 km) were established, with the innermost domain having a 2 km resolution across the Living Lab (Figure 23). Similar to Catalonia, the default 2 km resolution was employed, and in this case, complex terrain was a non-issue.

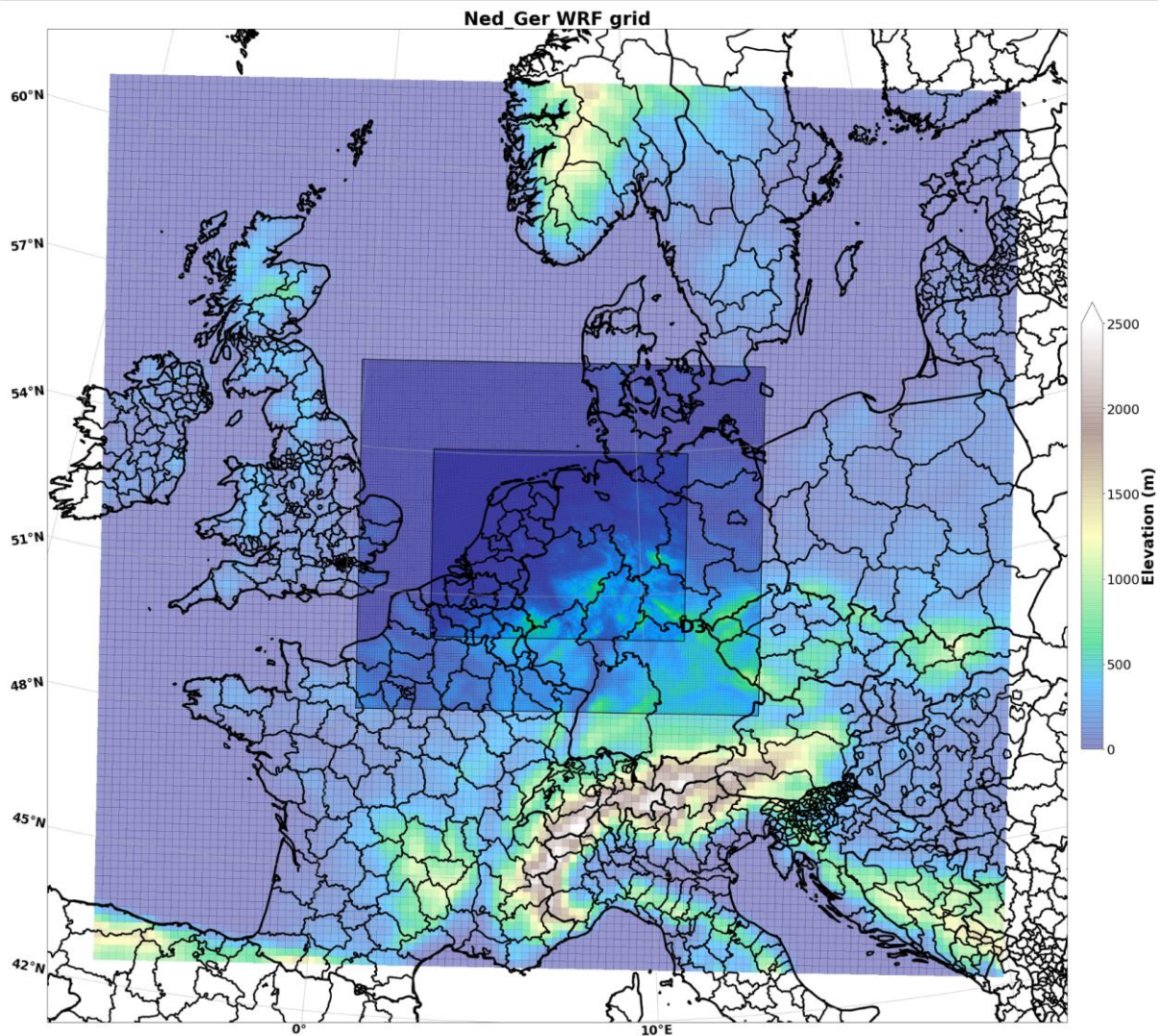


Figure 23 Netherlands-Germany WRF grids of 18, 6 and 2 km spatial resolution

- Gran Canaria Island Living Lab (Canary Islands)** was strategically captured with three nested domains (Figure 24). The resolutions downscaled from 9 km and 3 km capturing the entire Archipelago, to 1 km around Gran Canaria Island. Gran Canaria being small with complex topography required a 1 km resolution to capture the terrain appropriately. It is the highest resolution Living Lab designed to capture any complex inter-island weather interactions.

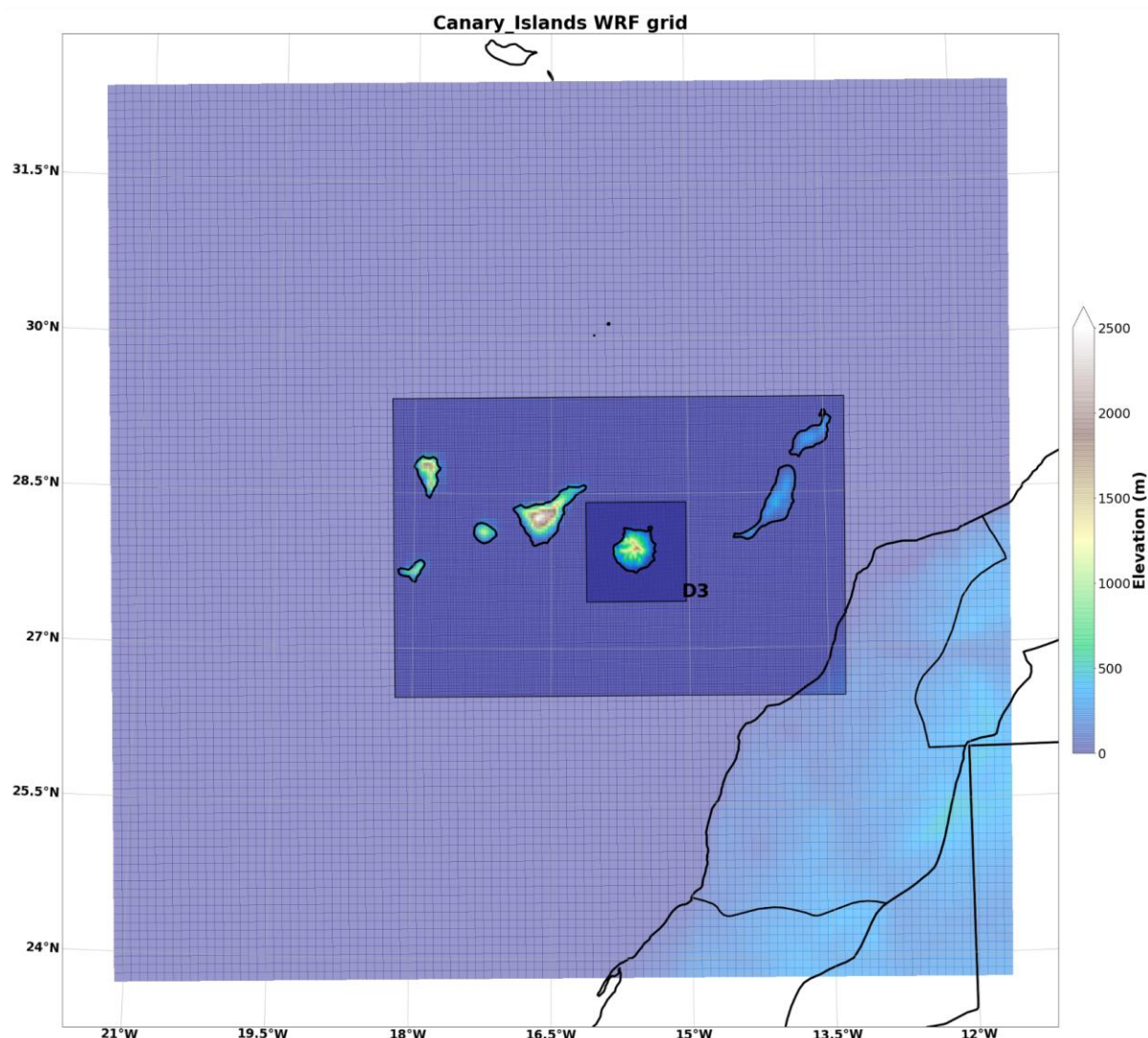


Figure 24 Gran Canaria Island WRF grid of 1 km (D3) and the Canary Islands grids of 3 km (D2) and 9 km (D1) spatial resolution

#### 4.3.2.2. Technosylva WRF metrics

For simulation optimization, Technosylva selected 45 raw variables to be included in the raw WRF output. Additional post-processing computed 12 variables with significance to fire weather and convective forecasting. The derived variables that are shown in the FIRE-RES ISS viewer (i.e., its corresponding label appears in brackets) are as follows:

- **Planetary Boundary Layer (PBL Height)**. It is the lowest layer of the troposphere where wind is influenced by friction. The thickness of the PBL is not constant. At night and in the cool season, the PBL tends to be lower in thickness while during the day and in the warm season, it tends to have a higher thickness.
- **Quantitative Precipitation Forecasts (Total QPF)**. It depicts the total amount of liquid precipitation expected to fall in a defined period of time. In the case of snow

or ice, QPF represents the amount of liquid that will be measured when the precipitation is melted.

- **Relative humidity at 2 metres above ground (2m AGL Relative Humidity).** A derived variable for atmospheric moisture that is commonly used in wildland fire due to its intuitive interpretation of atmospheric moisture. It measures the percentage of moisture the atmosphere holds compared to the maximum moisture possible.
- **Total Solar Irradiance (Solar Radiation).** The amount of solar radiation received at the top of the Earth's atmosphere.
- **Temperature at 2 metres above ground level (2m AGL Temperature).**
- **Vapour Pressure Deficit at 2 metres above ground level (2m AGL VPD).** A derived variable for atmospheric moisture that has been shown to correlate well with fuel moisture content. It measures the thirst of the atmosphere and the drying effect on the vegetation.
- **Wind speed at 10 metres above ground level (10m AGL Wind Speed).**
- **Convective temperature / triggering temperature (Convective Temperature).** The approximate temperature that the air near the ground must warm to for surface-based convection to develop, based on analysis of a sounding.
- **Cloud Cover Layer height (CCL Height).** It provides vertical cloud layer information. Cloud Layers are calculated and usually displayed as Low (below 10 kft), Mid (10-24 kft), High (above 24 kft), or a combination of these.
- **Surface-based Equilibrium level (Equilibrium Level).** The height above the level of free convection (LFC) at which the temperature of a rising air parcel again equals the temperature of the environment. It can estimate the minimum cloud top temperature (maximum vertical development of a convective column).
- **Surface-based Lifted Condensation Level (LCL Height).** It is the level at which a parcel becomes saturated if lifted adiabatically from the surface. It can be used as a reasonable estimate of cloud base height when parcels experience forced ascent.
- **Surface-based Level of Free Convection (LFC Height).** The level at which a surface parcel of air lifted dry-adiabatically until saturated and saturation-adiabatically thereafter would first become warmer than its surroundings in a conditionally unstable atmosphere.

Special considerations were taken in the WRF configuration selection. For fire weather forecasting, wind is the most critical and challenging to predict. Past studies have shown the Land Surface Model (LSM) and Planetary Boundary Layer (PBL) schemes to be the most impactful for wind forecasting (Cao & Fovell, 2018; Carvalho et al., 2020). Therefore, a proven configuration for fire weather forecasting options that have been tested and successfully utilised operationally in the western United States was utilised (Table 4). This

configuration had also validated well during the Lahaina Fire of 2023, which being an island chain is similar to the Gran Canaria Island. The WRF model was tested by means of other LSMs. The LSM has a large impact on near surface variables such as temperature and winds. Differences in surface roughness have large impact winds (Cao & Fovell 2018, Duine et al. 2019, among others).

*Table 4 List of the final parametrization for WRF layers, the scheme selected, and the nest option employed*

Parameterization	Scheme Selected	Nest specific option
Microphysics	Thompson	8, 8, 8
Cumulus	Kain-Fritsch	1, 1, 0
Radiation	RRTMG	4, 4, 4
Planetary Boundary Layer	MYNN level 3	6, 6, 6
Surface Layer	MYNN	5, 5, 5
Land Surface Model	NOAH-MP	4, 4, 4

#### 4.3.3. FireRisk assessment implementation process

For the calculation of the daily FireRisk metrics in the addressed LLs, the corresponding microservices have been deployed in the Azure Cloud environment. Four different types of Azure Cloud Service environment were used:

- Azure Container Apps – Used for deploying web applications that orchestrate the risk processes.
- Azure Blob Storage – Used for storing files such as the Network Common Data Form (NetCDF) files, risk files, LLs fuels scenario data and configurations related to the risk processes.
- Azure Container Jobs – Used for processes that require long execution time such as the creation of the H3 hexagons.
- Azure Batch – Used for running high resources demanding processes such as the risk processes.

The implementation workflow of the FireRisk module is based on the FIRE-RES infrastructure (included itself into the Azure infrastructure), allowing it to calculate several risk metrics at the same time, fitting perfectly the extent of the four LLs. Firstly, each WRF weather for each LL was used to run a parallel FireRisk execution and calculate each risk output. Each LL has its own pipeline execution but all of them follow the same scheme:

- Calculation of the Dead Fuel Moisture Content (DFMC) data by means of Nelson (2000) coupled differential formulas. It requires solar radiation, air temperature,

dew point temperature, and precipitation as inputs to determine trends in atmospheric dryness and vegetation greenness/growth.

- The Live Fuel Moisture Content (LFMC) results, calculated for each of the LLs, is added to the DFMC data. The LFMC which relies on different inputs including weather data (Vapour Pressure Deficit, precipitation, photoperiod, etc.), plant species, vegetation indexes captured with satellite-based sensors (e.g., Moderate Resolution Imaging Spectroradiometer - MODIS, Sentinel-2, Landsat 8) and phenology. Technosylva's LFMC model was trained through Machine Learning algorithms. Each LL has its own LFMC data that will be added to its corresponding weather file to later be included in the FireRisk calculations.
- The next step consists of creating a NetCDF file with all weather data in the Technosylva weather format, which is a common standard format for all Technosylva Applications to easily handle this kind of data. The weather variables that are required inside the NetCDF to run the risk processes are:
  - Relative humidity: - 0-1(ratio) \* 1,000.
  - Temperature: in °C \* 10.
  - Cumulative precipitation: in mm \* 1,000.
  - Dead Fuel Moisture 1h, 10h and 100h: - 0-1 (ratio) \* 1,000.
  - Live Fuel Moisture Herbaceous and Woody - 0-1(ratio) \* 1,000.
  - U-component of the wind in km/h \* 10.
  - V-component of the wind in km/h \* 10.
- Transform the fuel moisture metrics data from NetCDF format into a Hexagonal 3 (H3) spatial indexing system. These hexagonal cells, often referred to as "hexels", allow for efficient spatial indexing and querying by means of different resolutions or levels. For all LLs, the fuel moisture metrics data are aggregated to level 7 hexels, and risk data to level 8 hexels.
- All fuel moisture metrics data from different LLs are loaded and integrated into a common database for easily querying them.
- Once all fuel moisture metrics and scenario data (see section 4.4) are made available in the database, the FireRisk module is executed to calculate the risk metrics (see section 4.5.3).
- The final format of FireRisk metrics results as well as the fuel moisture data metrics are included in the H3 system. Ending with the loading of all risk and fuel moisture data into the common database.
- The Data Bases (DB) where the risk data is stored is a dedicated PostgreSQL DB created in Azure, one for the fire behaviour metrics and another DB that is used for the fuel moisture content metrics.
- As a middleware between the DB and the IS's Graphical User Interface (GUI), a tile server called *martin*<sup>1</sup> is used (Figure 25). *martin* exposes as vector tile services functions created in the PostgreSQL databases. These functions return the H3

---

<sup>1</sup> <https://martin.maplibre.org/>

geometries with the associated values of the variables. The geometries are then drawn and symbolised in the browser.

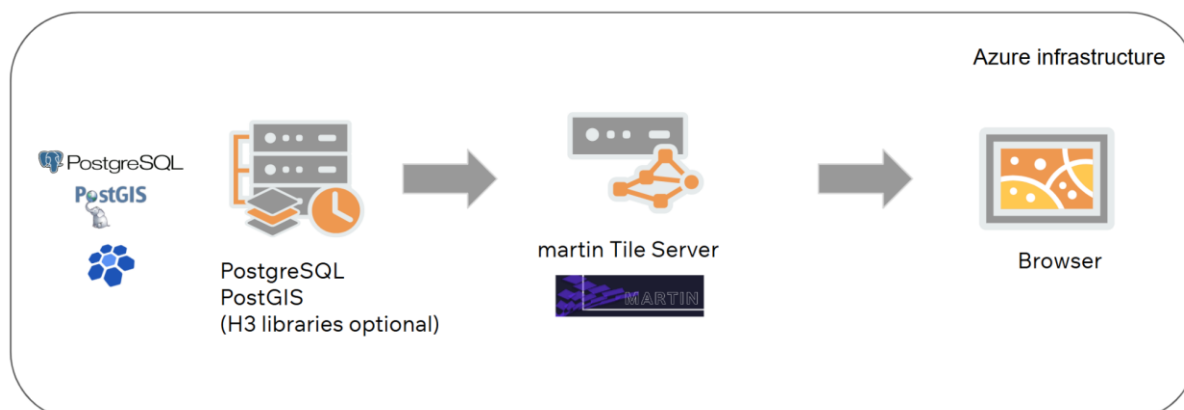


Figure 25 GIS services architecture

#### 4.3.3.1. FireRisk assessment outputs

FireRisk simulations main modules are Rothermel's (1972) surface model, Van Wagner's (1977) crown fire initialization and evolution model, spotting model based on Chase's (1984) maximum spotting distance for wind driven fires, and a wind adjustment model between different heights based on Andrews' (2012) work, and fire encroachment into urban areas (Figure 26). The time evolution is computed using a Minimum Travel Time algorithm (Finney, 2002) with up to 32 degrees of freedom (directions) that solves the Eikonal equation of a spreading curve  $\Gamma$  subject to the speed function  $ROS(\mathbf{x})$ :

$$|\nabla T| = 1 / ROS(\mathbf{x});$$

Where  $T(\mathbf{x})$  is the arrival time function, and  $ROS(\mathbf{x})$  the ROS of the fire in any possible direction at  $\mathbf{x}$ . This algorithm is similar to the well-known Dijkstra's (1959) algorithm but more adapted to grids instead of the original model that uses graphs. It provides the arrival time of the fire at each cell in the domain.

Encroachment is a critical component in the simulations as it affects the number of buildings and population impacted. To deal with complex urban areas, they have been classified into classes depending on their structure (roads, urban core, isolated, sparse) and their surrounding fuels, characterised as high versus low fire behaviour fuels). Specific encroachment factors can then be applied to each urban type which will affect the way the fire affects the urban area.

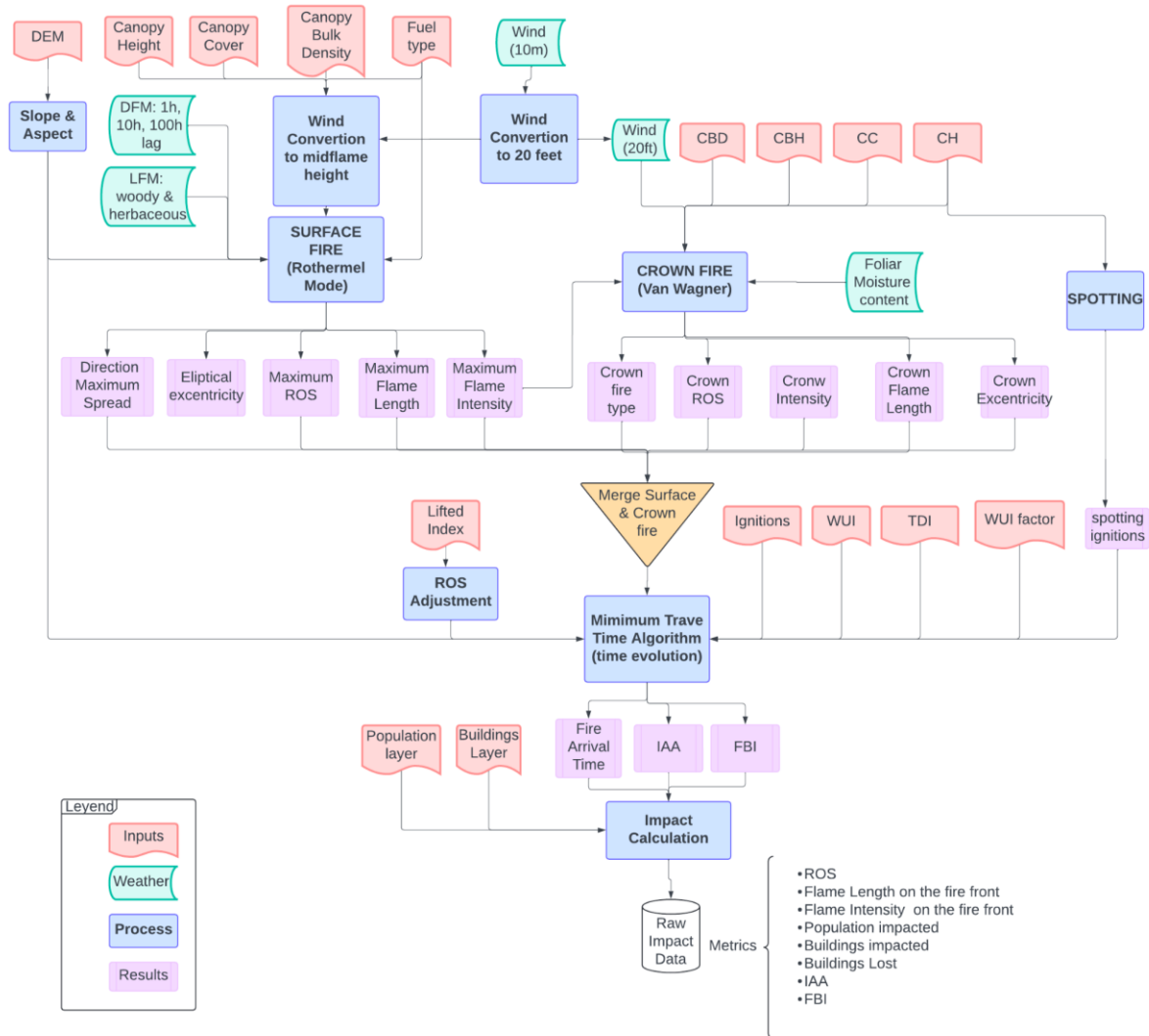


Figure 26 FireRisk module metrics estimation workflow

FireRisk metrics at the territorial level were calculated in all LLs for each 3-hours with a forecast of 96 hours. As mentioned before, the process starts with WRF hourly weather data as input to finally generate the following daily FireRisk metrics:

- **Rate of Spread.** This layer shows the rate of spread of the fire in m/min, i.e., the expected speed of the fire for each cell of the simulations (Figure 27).

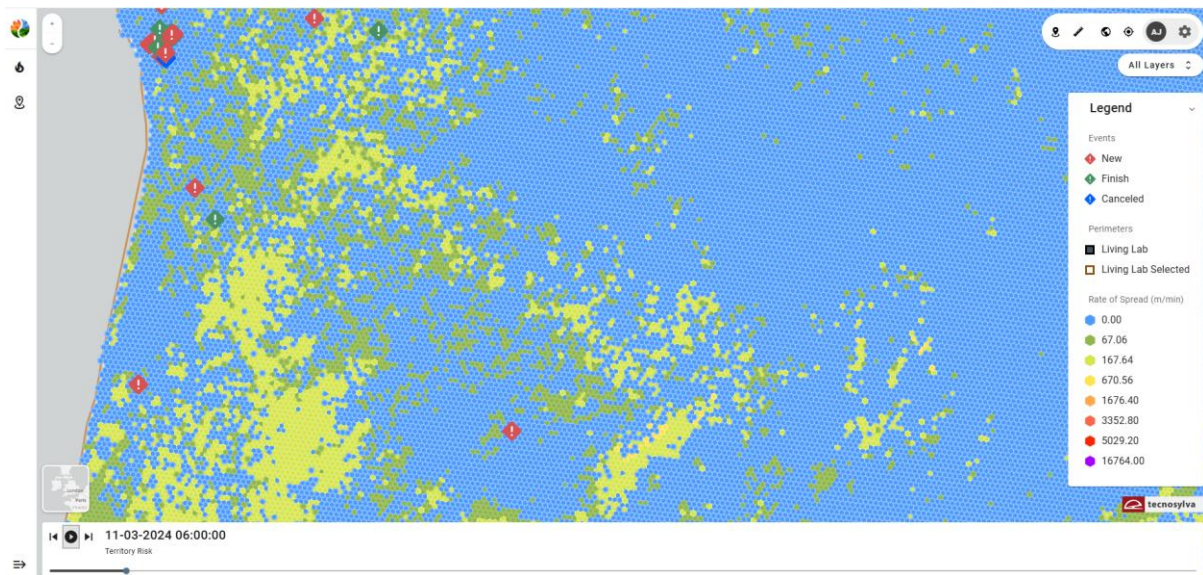


Figure 27 Rate of spread (m/min) as territory risk layer (h3) visualised in the ISP for the Portugal LL

- **Population Impacted.** Total population impacted by the simulation footprint.
- **Initial Attack Assessment Index.** It represents how difficult it is to contain or suppress a fire in the first 2 hours after ignition. It is a categorical indicator that ranges from 1 to 5, when the higher the value, the more active fire behaviour, the more complex the terrain, and thus the more likely it is for the initial attack to fail, posing a potential threat.
- **Flame Length.** It is the distance in metres measured from the average flame tip to the middle of the flaming zone at the base of the fire.
- **Fire Size Potential.** Total simulation size in hectares. The Fire Size Potential represents the actual simulated acreage of a fire based on the local fuels, weather, and terrain starting from an ignition at a specific location and time (Figure 28).

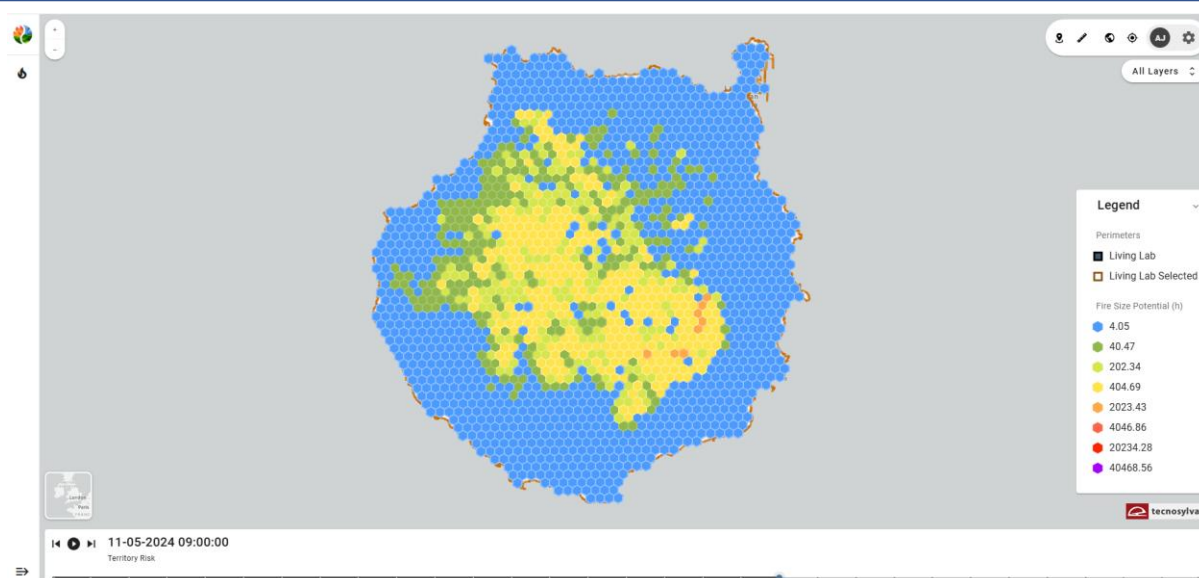


Figure 28 Fire size potential (ha) as territory risk layer (h3) visualised in the ISP for the Gran Canary Island LL

- **Fire Behaviour Index.** The Fire Behaviour Index (FBI) is a categorical indicator that ranges from 1 to 5 and is computed using the average Flame Length in metres and Rate of Spread (in km/h or m/min) on the fire front during the whole duration of the fire (the 8-hours unsuppressed fire simulation). Essentially it details how large and fast-moving the flames are over the burn duration.
- **Buildings Threatened.** Total number of buildings threatened by the simulation footprint.
- **EAA.** Extended Attack Assessment index quantifies the fire activity potential over the territory, aiming to assist operational decision-making to reduce fire threats and risks. EAA is a forecast product produced on a daily basis that theoretically estimates the expected number of VIIRs hotspots, calculated every 3 hours at different hexel-based (h3) resolutions.

Technosylva fuel moisture calculations also utilise the WRF model as input to the **Nelson dead fuel moisture model**, which is widely accepted across the fire behaviour modelling community. The dead fuel moisture results have 2 km spatial resolution, and the resulting classifications represent the time lag it takes for a fuel's moisture content to reach equilibrium with its environment. The following dead fuel moistures are forecasted at the territorial level:

- **Dead Moisture 1h.** 1-hour fuels are the fine dead fuels, with diameters less than 0.25", such as grasses. The moisture contents in percentage of 1-hour fuels respond quickly (within minutes) to changing weather conditions (Figure 29).

- **Dead Moisture 10h.** 10-hour fuels are small dead fuels, with diameters ranging from 0.25" to 1". The moisture contents in percentage of 10-hour fuels respond quickly to changing weather conditions, but not as quickly as the 1-hour fuels.
- **Dead Moisture 100h.** 100-hour fuels are standard dead fuels, with diameters ranging from 1" to 3". Due to the larger size, the moisture content in percentage of 100-hour fuels responds slower to changing weather conditions. 100-hour fuels can be used to estimate the average moisture content of the forest floor.

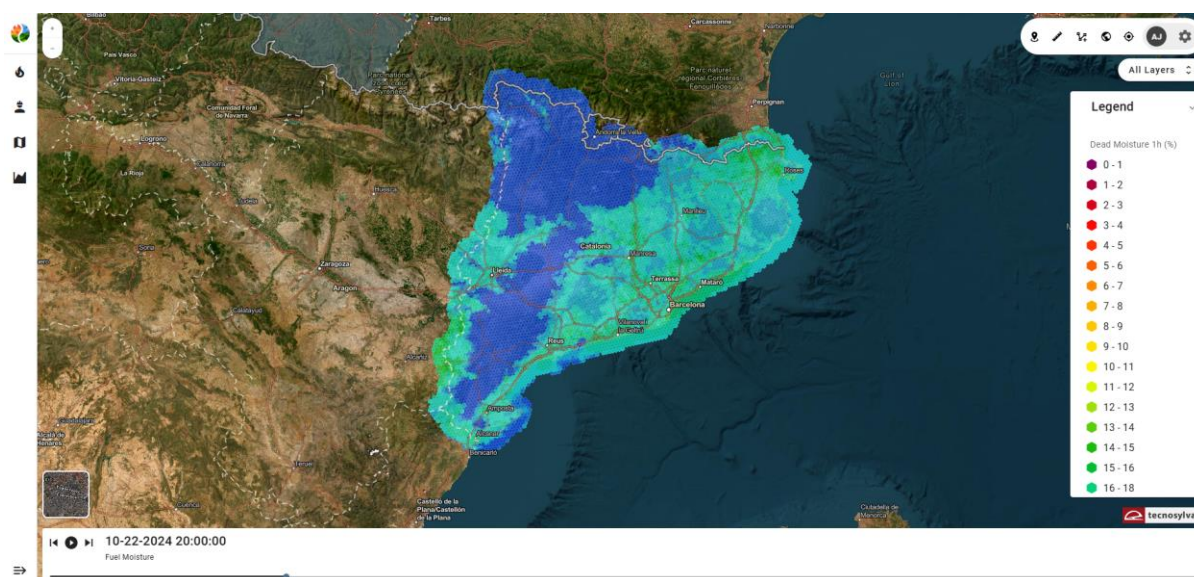


Figure 29 Dead Moisture 1h (%) as fuel moisture metric (h3) visualised in the ISP for the Catalonia LL

The **live fuel moisture** products are derived from a machine learning proprietary model developed by Technosylva that ingests satellite observations and in-situ observations. Live fuel moisture differs from herbaceous fuels and woody fuels, primarily due to phenological differences. These percentages are defined by the National Wildfire Coordinating Group (NWCG), so the flammability range extends from about 35 percent to over 200 percent in living vegetation, and about 1.5 to 30 percent for dead fuels. The metrics are updated weekly at the territorial level and includes:

- **Woody LFM (TSYL, 2020).** Woody Live Fuel Moisture (shrubs and trees) in percentage.
- **Herbaceous LFM (TSYL, 2020).** Herbaceous Live Fuel Moisture (primarily grasses) in percentage.

More details about the FireRisk implementation into the ISP have been included in the Deliverable "D5.2".

#### 4.3.4. FireSim implementation process

FireSim implements a RESTful API serving as a bridge between the GUI and the FireSim simulation core that calculates all sims run by the users in every LL. The API implements Hangfire as a system of handling simulation runs and enqueueing all runs requested by the LLs (i.e., jobs).

This RESTful API is published on a Windows Server machine located in a Microsoft Azure Cloud environment, where the FireSim Core is also located and run. The FireSim core is the central component of FireSim, where all the simulation processes are run and the results are created. The central database for FireSim is stored in a Linux server machine located also in a Microsoft Azure Cloud environment that serves as a data repository for the API.

A typical complete workflow when running a sim would be like this:

- A user launches a simulation from any of the LL environments. The LL relays a series of POST requests to work with the API in the process of running and retrieving simulations and their information. The requests involved in the process are listed below:
  - <https://stgfireresapifirecast.wildfireanalyst.com/api/simulation/SimulateJSON> - Launches a simulation.
  - <https://stgfireresapifirecast.wildfireanalyst.com/api/simulation/GetJobStatus> - Gets information on the job associated with the simulation run.
  - <https://stgfireresapifirecast.wildfireanalyst.com/api/simulation/GetSimulationStatus> - Gets information on the simulation process status.
  - <https://stgfireresapifirecast.wildfireanalyst.com/api/simulation/getsimulationsbySimStartTimedates> - Requests all available sims between two given dates for each of the LLs.
- The FireSim API runs several validation and input format checks before actually sending the request to the core.
- After checking the inputs, the NetCDF file for the selected date in the LL is downloaded from the BLOB storage to which it was uploaded by FireRisk.
- Simulation run begins. The simulation core may return a warning in case no spread fire is achieved, or a successful series of outputs matching the simulation mode selected in the LL.
  - <https://stgfireresapifirecast.wildfireanalyst.com/api/simulation/Getoutput> - Requests any of the simulation output files in any given format available.
- Simulation outputs are finally stored in the FIRE-RES Binary Large Object (BLOB) storage.

##### 4.3.4.1. FireSim outputs

The FireSim implemented in the FIRE-RES Integrated System includes a list of outputs after the technical process of development. Regarding the simulation modes, there are

two available options with their corresponding simulation results: standard propagation and probabilistic mode.

### Standard Propagation mode

FireSim has the ability to generate conventional fire behaviour outputs based on specific ignition location points. The fire simulation results provided are:

- **Arrival Time.** Fire spread prediction depicts a raster fire perimeter representing fire time of arrival for each cell.
- **Rate Of Spread.** This layer shows the expected speed (m/min) of the fire for each cell of the simulation.
- **Flame Length.** This layer represents the simulated height of the flames in metres.
- **Crown Fire Type.** This layer shows the simulated fire type: 0 = Surface fire, 1 = Conditional Crown type, 2 = Torching and 3 = Crowning.
- **Fire Paths.** This layer represents the probability of fire progression trajectories according to three categories: the main are those paths over 0.65 (i.e., 65% of likelihood), the secondaries are those over 0.50 (i.e., 50% of likelihood), and the rest are those over 0.25 (i.e., 25% of likelihood).
- **Initial Attack Assessment (IAA).** It is a dynamic and categorical risk indicator that aims to evaluate the difficulties to the response teams during the first 1-2 hours after ignition time. Its values range from 1 to 5. In the ISS viewer, IAA is accompanied by other two metrics: **Size (1hr)** and **Avg. Slope**, which means the fire size in m<sup>2</sup> reached within the first hour of the simulation, and the mean slope value in percentage within the simulated perimeter, respectively.
- **Fire Behaviour Index (FBI).** It is a dynamic and categorical indicator that measures the potential intensity, severity and spread of a new fire. It is the result of combining the fire's potential Flame Length (FL) and Rate of Spread (ROS). FBI ranges from 1 to 5, so the higher the value, the more active fire behaviour. In the ISS viewer, FBI is accompanied by the variables employed to calculate it: **Flame Length** and **ROS** (both already described above). Note that for the case of this ROS, the units are expressed in km/h.
- **Growth Potential Index (GPI).** This categorical index uses the fire perimeter in kilometres for the first hour of fire growth with no intervention of suppression resources and fire area growth in percentage from the area of a fire spread simulation two hours after simulation started divided by the fire size in the first hour. The different values of GPI vary from 1 (Low) to 5 (Extreme). In the IS viewer, GPI is accompanied by the variables used to obtain it: **Perimeter (1hr)** as the simulated fire perimeter in the first hour and, **Area (a2/a1)** as the ratio between the burned area in the 2 first hours and the first hour of the simulation.
- **Buildings impacted.** This layer shows the number of total buildings impacted by a specific simulation perimeter.
- **Population impacted.** This layer represents the total population impacted by a specific simulation perimeter.

One functionality related to Standard Propagation mode is the “adjustment mode”. After conducting a Standard simulation, control points during simulation can be designed to make customizer adjustments. Concretely, it consists of adjusting the simulated fire growth to match the observed fire progression. Adjusting the ROS parameters is a typical technique to reduce simulation inaccuracies. These adjustment factors are conducted in the following way:

$$ROS_{final} = Adj_{fuel} \times ROS_{model}$$

Where *Adj<sub>fuel</sub>* is a set of fuel related constants used to modify fire’s ROS in a simulation. Fire practitioners and researchers are familiar with these factors because they offer a straightforward method of matching fire simulations to actual observed fire spread. Nevertheless, manually finding these factors is a difficult and time-consuming task that calls for perseverance and a good number of trial-and-error attempts to be finished.

A collection of control points or lines with the actual fire's arrival time known serves as the adjustment data. These points shall be inserted by the user through the FIRE-RES GUI. As is specified in deliverable D5.2, this functionality has been implemented in FireSim for FIRE-RES and the integration will occur in the next months. This adjustment technique is based on minimising the error between the simulated fire growth and the actual fire by identifying the optimal ROS adjustment variables (Rothermel, 1983) using a least squares approach.

### Probabilistic mode

Probabilistic mode uses a Monte Carlo method to run 50 simulations using the input data and will overlay all simulation outputs together to create a probabilistic surface. This mode also considers the ROS adjustment based on the Lifted Index. In addition, it provides the ability to adjust a variability on four inputs within a range of acceptable values:

- Wind direction (degrees).
- Wind speed (km/h).
- 1 hr Fuel Moisture (%).
- Live Woody and Herbaceous Fuel Moisture (%).

The fire simulation results provided in the Probabilistic mode are different from the Standard Propagation mode, mainly because of the higher variability of the ranges used in the inputs previously defined by the user. Apart from that, the Probabilistic mode does not obtain Crown Fire Type and Fire Paths outputs, but a new output layer called **Probabilistic**, which represents the likelihood in percentage of the simulated perimeter.

## 5. Technology Readiness Level (TRL)

Two main forest fire technologies are addressed inside the IA 5.2, one is the simulator ForeFire developed by CNRS and another is the Wildfire Analyst simulation capabilities developed by Technosylva. In the case of the CNRS ForeFire simulator (specified in the Deliverable D5.3), the advances have been materialised into the development and testing of a coupled fire-atmosphere spread model to consider the effect of pyro convection in fire behaviour, progression, and impact estimations. It has included the validation of EWE erratic propagation due to pyro convection or extreme winds through large scale coupled fire/weather simulation re-analyses on several extreme large fires in Europe since 2010. Plume and smoke in-drafts will also be qualified through numerical tools. The European Centre for Medium-Range Weather Forecasts (ECMWF) as well as enhanced high-resolution weather models (WRF) have been employed.

Technosylva's Wildfire Analyst simulator has been able to progress from TRL5 to TRL7 by adapting/adjusting the fire spread and behaviour on the use of EWEs simulation capability in operational models. For this commitment, the main milestone has been a new adjustment of the rate of spread by the addition of the lifted index (i.e., information related to instability of the atmosphere) to improve the simulation of the behaviour and conditions of EWEs. Additionally, indexes, such as IAA (Initial Attack Assessment) and EAA (Extended Attack Assessment), to predict the probability of the occurrence of likely EWEs have been developed and already implemented in several LLs. In the future, these indexes will be validated by applying these tools to ongoing potential EWEs occurring for each LL.

## 6. Conclusions

The main findings of this deliverable derived from the analyses of the EWEs drivers can be summarised as follows:

- A positive trend was observed between fire spread and wind speed, which decreased towards higher wind classes. Also, the rate of spread increases under unstable atmospheric conditions, especially at 500 hPa and when lifted index is between -6 and -2. In addition, the fastest vectors are those in convective conditions (i.e., Convective Flag < 8).
- Regarding the relationships between the Rate of Spread (ROS) and Convective Available Potential Energy (CAPE), the threshold of 1000 J/kg greatly defines fire propagation spreads (i.e., over that value a double of ROS vectors were found in moderate and high instability compared to those under stable conditions). Additionally, an exponential increase of the mean ROS was detected when wind gusts were greater.
- The validation of WFA simulated ROS correctly matched with the FireGuards' ROS values, despite the fact that the ROS patterns are more difficult to model and predict under unstable conditions. Thus, proving the model's ability to predict the average ROS in moderate-long fire runs.

Regarding the results of the FireSim module, one of the main highlights is that the fire simulation model was updated, including the lifted index, by means of an adjusted formulation of the ROS. This implementation affects both deterministic and probabilistic simulations. In terms of forecast weather that ingest the FireSim, Weather Research and Forecasting (WRF) was employed to show a high-resolution and daily meteorological prediction of four days for the four Living Labs. In order to optimise fire simulation, Technosylva computed 12 significant variables for fire weather and convective forecasting. Additionally, different WRF configurations were tested to improve the fire weather forecasting (especially the wind prediction). Finally, daily FireRisk metrics at the territorial level for each Living Lab have been implemented. On one hand, 8 variables related to potential fire behaviour and initial-extended attack difficulty; and on the other hand, 5 variables related to dead and live fuel moisture content have also been implemented.

## 7. References

- Andrews, P. L. (2012). Modeling wind adjustment factor and midflame wind speed for Rothermel's surface fire spread model (General Technical Report RMRS-266; p. 39). USDA Forest Service, Rocky Mountain Research Station.
- Campos, C., Couto, F. T., Filippi, J.-B., Baggio, R., & Salgado, R. (2023). Modelling pyro-convection phenomenon during a mega-fire event in Portugal. *Atmospheric Research*, 290, 106776. <https://doi.org/10.1016/j.atmosres.2023.106776>.
- Cao, Y., & Fovell, R. G. (2016). Downslope Windstorms of San Diego County. Part I: A Case Study. *Monthly Weather Review*, 144(2), 529–552. <https://doi.org/10.1175/MWR-D-15-0147.1>
- Cao, Y., & Fovell, R. G. (2018). Downslope Windstorms of San Diego County. Part II: Physics Ensemble Analyses and Gust Forecasting. *Weather and Forecasting*, 33(2), 539–559. <https://doi.org/10.1175/WAF-D-17-0177.1>
- Carvalho, L., Duine, G.-J., Jones, C., Zigner, K., Clements, C., Kane, H., Gore, C., Bell, G., Gamelin, B., Gomberg, D., Hall, T., Jackson, M., Dumas, J., Boldt, E., Hazard, R., & Enos, W. (2020). The Sundowner Winds Experiment (SWEX) Pilot Study: Understanding Downslope Windstorms in the Santa Ynez Mountains, Santa Barbara, California. *Monthly Weather Review*, 148(4), 1519–1539. <https://doi.org/10.1175/MWR-D-19-0207.1>
- Chase, C. H. (1984). Spotting Distance from Wind-Driven Surface Fires—Extensions of Equations for Pocket Calculators (INT-346; p. 21). USDA Forest Service, Intermountain Forest and Range Experiment Station.
- Di Giuseppe, F., Vitolo, C., Krzeminski, B., Barnard, C., Maciel, P., & San-Miguel, J. (2020). Fire Weather Index: The skill provided by the European Centre for Medium-Range Weather Forecasts ensemble prediction system. *Natural Hazards and Earth System Sciences*, 20(8), 2365–2378. <https://doi.org/10.5194/nhess-20-2365-2020>.
- Dijkstra, E. W. (1959). A note on two problems in connexion with graphs. *Numerische Mathematik*, 1(1), 269–271.
- Duine, G.-J., Jones, C., Carvalho, L. M. V., & Fovell, R. G. (2019). Simulating Sundowner Winds in Coastal Santa Barbara: Model Validation and Sensitivity. *Atmosphere*, 10(155), 21. <https://doi.org/doi:10.3390/atmos10030155>.
- Fernandes, P., Gonçalves, H., Loureiro, C., Fernandes, M., Costa, T., Cruz, M. G., &

- Botelho, H. (2009). Modelos de Combustível Florestal para Portugal. Actas Do 6o Congresso Florestal Nacional. SPCF, 348–354.
- Filippi, J. B., Bosseur, F., Mari, C., Lac, C., Le Moigne, P., Cuenot, B., Veynante, D., Cariolle, D., & Balbi, J. (2009). Coupled Atmosphere-Wildland Fire Modelling. *Journal of Advances in Modeling Earth Systems*, 1(4), JAMES.2009.1.11. <https://doi.org/10.3894/JAMES.2009.1.11>
- Filippi, J.-B., Bosseur, F., Pialat, X., Santoni, P.-A., Strada, S., & Mari, C. (2011). Simulation of Coupled Fire/Atmosphere Interaction with the MesoNH-ForeFire Models. *Journal of Combustion*, 2011(1), 540390. <https://doi.org/10.1155/2011/540390>
- Finney, M. A. (2002). Fire growth using minimum travel time methods. *Canadian Journal of Forest Research*, 32(8), 1420–1424. <https://doi.org/10.1139/x02-068>
- Gonzalez-Olabarria, J. R., Carrasco, J., Pais, C., Garcia-Gonzalo, J., Palacios-Meneses, D., Mahaluf-Recasens, R., Porkhum, O., & Weintraub, A. (2023). A fire spread simulator to support tactical management decisions for Mediterranean landscapes. *Frontiers in Forests and Global Change*, 6. <https://doi.org/10.3389/ffgc.2023.1071484>.
- Hersbach, H, Bell, B., Berrisford, P, Biavati, G, Horányi, A, Muñoz Sabater, J, Nicolas, J, Peubey, C, Radu, R, Rozum, I, Schepers, D, Simmons, A, Soci, C, Dee, D, & Thépaut, J-N. (2023). ERA5 hourly data on single levels from 1940 to present. Copernicus Climate Change Service (C3S) Climate Data Store (CDS) [Dataset]. <https://doi.org/10.24381/cds.adbb2d47>.
- Kutchartt, E., González-Olabarria, J. R., Aquilué, N., Garcia-Gonzalo, J., Trasobares, A., Botequim, B., Hauglin, M., Palaiologou, P., Vassilev, V., Cardil, A., Navarrete, M. Á., Orazio, C., & Pirotti, F. (2024). Pan-European fuel map server: An open-geodata portal for supporting fire risk assessment. *Geomatica*, 100036. <https://doi.org/10.1016/j.geomat.2024.100036>.
- Kutchartt, E., González-Olabarria, J., Trasobares, A., Aquilué, N., Guerra-Hernández, J., Nunes, L., Sequeira, A., Botequim, B., Hauglin, M., Palaiologou, P., Cardil, A., Rogai, M., Vassilev, V., Pimont, F., Martin-Ducuo, O., & Pirotti, F. (In Press). Satellite-based mapping of canopy fuels at the pan-European scale. *Geo-Spatial Information Science*. <https://www.zotero.org/google-docs/?34PNUx>
- Mendes, M., Cardil, A., Moratiel, I., Lorea, G., Rosel, M., Rego, F., Nunes, L., Sequeira, C., Dias, D., Botequim, B., Viana, M., Barcons, J., Filippi, J., Gliner, M., & Corbera, J. (2022). FIRE-RES Technical requirements and system architecture of the

- integrative software system (Deliverable D5.1 FIRE-RES project; p. 65).  
10.5281/zenodo.7330664.
- Nelson, R. M. (2000). Prediction of diurnal change in 10-h fuel stick moisture content. *Canadian Journal of Forest Research*, 30, 1071–1087.  
<https://doi.org/10.1139/x00-032>.
- Ntinopoulos, N., Spiliotopoulos, M., Vasiliades, L., & Mylopoulos, N. (2022). Contribution to the Study of Forest Fires in Semi-Arid Regions with the Use of Canadian Fire Weather Index Application in Greece. *Climate*, 10(10), Article 10.  
<https://doi.org/10.3390/cli10100143>.
- Pinto, M. M., DaCamara, C. C., Hurduc, A., Trigo, R. M., & Trigo, I. F. (2020). Enhancing the fire weather index with atmospheric instability information. *Environmental Research Letters*, 15(9), 0940b7. <https://doi.org/10.1088/1748-9326/ab9e22>.
- Recasens, R. M., Carrasco, J., Lisón, F., Pais, C., Miranda, A., de la Barra, F., & Weintraub, A. (2022). Combining optimization and fire simulation modeling to protect biodiversity values at a landscape scale. 2022 IEEE Latin American Conference on Computational Intelligence (LA-CCI), 1–6. <https://doi.org/10.1109/LA-CCI54402.2022.9981527>.
- Rothermel, R. C. (1972). A mathematical model for predicting fire spread in wildland fuels (Research Paper INT-115). USDA Forest Service, Intermountain Forest and Range Experiment Station.
- Rothermel, R. C. (1983). How to Predict the Spread and Intensity of Forest and Range Fires (p. 164) [General Technical Report INT-143]. USDA Forest Service, Intermountain Forest and Range Experiment Station.
- Scott, J. H., & Burgan, R. E. (2005). Standard fire behavior fuel models: A comprehensive set for use with Rothermel's surface fire spread model (RMRS-GTR-153; p. RMRS-GTR-153). U.S. Department of Agriculture, Forest Service, Rocky Mountain Research Station. <https://doi.org/10.2737/RMRS-GTR-153>.
- Tory, K. J., & Kepert, J. D. (2021). Pyrocumulonimbus Firepower Threshold: Assessing the Atmospheric Potential for pyroCb. *Weather and Forecasting*, 36(2), 439–456.  
<https://doi.org/10.1175/WAF-D-20-0027.1>
- Van Wagner, C. E. (1977). Conditions for the start and spread of crown fire. *Canadian Journal of Forest Research*, 7(1), 23–34. <https://doi.org/10.1139/x77-004>.



**FIRE-RES**